NASA LEWIS SEMI–ANNUAL STATUS REPORT
NAG 3–67 (6/2/80 -- 11/30/80)

PREDICTION OF SOUND RADIATED FROM DIFFERENT PRACTICAL JET ENGINE INLETS

By

B. T. Zinn
W. L. Meyer

GEORGIA INSTITUTE OF TECHNOLOGY
SCHOOL OF AEROSPACE ENGINEERING
ATLANTA, GEORGIA 30332

1980

NASA LEWIS SEMI-ANNUAL STATUS REPORT

NAG 3-67 (6/2/80 - 11/30/80)

PREDICTION OF SOUND RADIATED FROM DIFFERENT PRACTICAL JET ENGINE INLETS

By

B. T. Zinn

W. L. Meyer

SCHOOL OF AEROSPACE ENGINEERING

GEORGIA INSTITUTE OF TECHNOLOGY

ATLANTA, GA. 30032

ABSTRACT

This report summarizes the work performed during the first six months of a NASA-Lewis sponsored research program (Contract Number NAG 3-67). This research program is concerned with the calculation of the far field radiation patterns surrounding various practical jet engine inlet configurations under different excitation conditions. This initial phase of the research program is primarily concerned with the upgrading of existing computer codes. These computer codes are based on a special integral representation of the external solutions of the Helmholtz equation and they are capable of calculating the sound field radiated from general axisymmetric bodies with complex boundary conditions up to non-dimensional wave numbers of ten (based on radius) with less than ten percent error in the acoustic quantities of interest.

During the past six months the computer codes have been refined and expanded so that they are now more efficient computationally by a factor of about three and they are now capable of producing accurate results up to non-dimensional wave numbers of twenty. Computer programs have also been developed to help generate accurate geometrical representations of the inlets to be investigated. This data is required as input for the computer programs which calculate the sound fields. This new "geometry generating" computer program considerably reduces the time required to generate the input data which was one of the most time consuming steps in the process.

The results of sample runs using the NASA-Lewis QCSEE inlet are presented and comparison of run times and accuracy are made between the old and upgraded computer codes. The overall accuracy of the computations is determined by comparison of the results of the computations with simple source solutions.

TABLE OF CONTENTS

INTRODUCTION

This research program consists of two major tasks. The first task is concerned with the upgrading and testing of the computer codes and the second is concerned with the calculation of the radiation patterns for specific inlet configurations. This report describes the progress made to date on the completion of the first task.

The computer programs previously developed are capable of predicting the sound field radiated by various geometrical configurations. The theoretical basis for these programs is presented in Refs. 1-3 (See Appendix A for Ref. 3). These publications describe the development of a unique integral formulation of the acoustic radiation problem and its application in the calculation of 2-D, 3-D and cylindrically symmetric radiation patterns. In the present investigation the cylindrically symmetric form of the equations[3] is employed as the inlet geometries we are concerned with in this study are all axisymmetric.

The computer codes developed for the calculation of radiation patterns about an axisymmetric body were initially developed for calculations at relatively low non-dimensional wave numbers (i.e., less than 10) and thus were not as efficient as they could be. To calculate results for higher wave numbers (i.e., up to 20) the computer codes had to be upgraded so that more calculation points could be handled on the bodies; and, to keep the calculation times reasonable the computer codes had to be made more efficient. Also, in using these "old" computer codes considerable time was required for the specification of the body geometry and boundary conditions (i.e., the input data). To expedite the input process computer codes had to be developed to generate the input data in a form which could be directly input

into the "new" computer codes.

Once the computer codes were upgraded they were tested for speed and accuracy. To test for speed the upgraded programs were simply compared to a bench mark set of computer runs done with the old computer codes for the "QCSEE"[4] inlet previously studied for the Air Force[5-6]. The accuracy of the computer codes was checked by comparison of the calculated solutions to those generated by simple sources. The method of using a simple source to generate and check solutions for complex geometries is detailed in Ref. 3(See Appendix A.).

The particular form of the equations used in this study is termed cylindrically symmetric as the solutions describing the radiation patterns from the axisymmetric inlets may have tangential dependence. In this case, the radiation patterns may be calculated separately for any tangential mode; and, since each tangential mode must be solved for separately there is no coupling between them. Also, since the equations are linear, as many tangential mode solutions as required may be calculated and these modal solutions may be summed. For each tangential mode all radial modes (both cut-on and cut-off) are automatically considered and thus the theory does allow coupling between the various radial modes present for each tangential mode. That is, if a particular radial mode is present at the driver (i.e.,the fan) plane but it is above cut-off for the duct the theory shows that it dies out exponentially as it should.

In this study tangential mode numbers, M, of up to 13 are considered with corresponding non-dimensional wave numbers of up to 20. Since the cut-off frequency for the first radial mode of the 13th tangential mode is

approximately ka = 14.92837 (where k is the wave number and a is the characteristic body dimension -- typically the duct radius at the driver plane) the cut-off ratio is of the order of 1.3. The limiting factor is the non-dimensional wave number so that higher cut-off ratios may be achieved for lower tangential mode numbers. In this connection it should be pointed out that during the first half of this contract period computer programs have also been developed to calculate the non-dimensional cut-off wave numbers for any tangential and radial mode and to calculate the mode shapes for these conditions.

EFFICIENCY AND ACCURACY OF THE COMPUTER CODES

The original computer codes were used to produce bench mark runs for comparison purposes. One of these runs (which is representative) was made for the case where there were 105 points on the surface of the QCSEE inlet (See Appendix A for geometry.) at a non-dimensional wave number of ka = 10.0 and a tangential mode number of M = 10. The acoustic velocity for a simple source was specified on the surface of the body and the acoustic potential was calculated. The calculation of the distribution of the acoustic potential on the surface of the body required 867 sec. and the average absolute errors in its modulus and phase were found to be 14.4% and 33.0% respectively. With this data available a separate program is then used to calculate the acoustic potential at points in the field surrounding the body. Since this program involves a straight forward summation, not much optimization could be done on it. Thus, most of the optimization work was directed towards the program which calculates the acoustic quantities on the surface of the body. This surface program contains an NxN matrix (where N is the number of points on the body) that must be filled and solved to generate the surface quantities. Therefore, the computing time for the surface quantities go up roughly as the square of the number of points on the body which can become very significant for large N.

Much of the work in this area was directed simply towards generating a more efficient computer code, and significant gains were made. Also, different numerical integration methods were tested along with different matrix solving schemes; however, these were not as fruitful. For example,

different integration schemes such as Filon integration[7] were tried in the circumfrential, θ , direction. Compared to the presently used Gauss-Legendre integration scheme they were found to be no better and in most cases worse. Also, different matrix solvers such as Gauss-Seidel iteration with both over and under relaxation were tested and it was found that in order to maintain the accuracy obtained with the presently used Gauss-Jordan matrix reduction scheme too may iteration steps were required.

Some very minor changes to the computer codes such as adding the normals to the body at all the integration points within an integration sub-interval, yielded dramatically better results. It was also found that specifying the distance in the Gauss-Legendre integration formula in the θ direction in reverse order (i.e., starting at 180^{o} instead of 0^{o}) yielded better results. Neither of these charges increased computing time significantly but they were found to be responsible for much better accuracy.

New computer runs were then made for the same cases as the original bench mark set. For the representitive runs mentioned at the begining of this section (i.e. ka = 10.0, M = 10, 105 points on the surface of the QCSEE inlet with the normal acoustic velocity specified everywhere) the run time required for the surface solution of the acoustic potential decreased by almost a factor of 3 from 867 to 309 sec. Also, the average absolute percent errors in the modulus and phase of the computed acoustic potential on the surface of the inlet decreased from 14.4% and 33.0% to 9.4% and 10.3% respectively.

UPGRADING OF THE COMPUTER CODES

The second effort during the reporting period was concerned with the upgrading of the computer codes so that better accuracy could be obtained at higher non-dimensional wave numbers. This was done by the addition of more points on the surface of the body. It was expected that this effect would be linear in that twice the number points on the body should halve the error in the potential calculated on the body.

Another set of computer runs were then performed with 156 points on the surface of the QCSEE inlet. The increase in the required computer time should fall between $1/3\ N^3$, the operation count for the matrix solution via Gauss-Jordan reduction, and N^2, the number of terms that must be calculated to fill the matrix. This being the case the run time should fall between 681 sec. and 1013 sec.. For the representative case of M = 10 and ka = 10.0 the run time was in fact found to be 791 sec. which is less than the original bench mark runs of 867 sec. for the same case with only 105 points.

The average absolute percent errors in the modulus and phase of the potential on the surface of the body were found to be 8.7% and 93.5% respectively. In this connection one should note that although the average absolute percent error in the modulus of the acoustic potential decreased it did not decrease as much as expected and the error in the phase actually went up 9 times.

This anomoly was found to be due to the way in which the error was calculated; that is, the percent error was very small where the values of the potential were high but with the same magnitude error the percent errors were very high when the potential was small. Upon studying the results of

various runs it was found that the magnitude of the error remained almost constant over the entire body and thus a better measure of the error would be the normalized average absolute error in percent. It should be pointed out that this will be a departure from the way in which the errors were calculated in the past (i.e.,in the proposal for this research) and therefore previous error estimates can not be compared directly with these. It is also felt by the authors that this is a more reasonable way to calculate the error as the high tangential mode numbers whose characteristics are of interest in this study have solutions that tend to vary over many orders of magnitude. As an example of this, the solution for the acoustic potential on the surface of the inlet for the simple source case where M = 10 and ka = 10.0 varies from zero at the centerline of the inlet to $\mathcal{O}(10^{16})$ near the fan plane on the centerbody. The formula for the normalized average absolute error in percent is given by:

$$E = \left(\sum_{i=1}^{N} | (\varphi_{EXACT} - \varphi_{CALC}) | / N \right) X \left(\frac{100.0}{\varphi_{MAX}} \right) \qquad (1)$$

These errors, for the modulus and phase of the acoustic potential calculated on the surface of the inlet, were then recalculated for the representative bench mark run (i.e., M = 10, ka = 10.0, 105 points on the surface of the body) and were found to be 0.139% and 8.75% respectively. These errors were also calculated for the results generated by the improved computer code again using 105 points on the surface of the body and they were found to be 0.0999% and 3.10%, respectively. Finally, these same error estimates were made for the case where 156 points were used on the

surface of the body and they were found to be 0.0679% and 2.59%. As can be seen these error estimates show that the error is decreased by about a third as is expected when the number of points is increased by about a half. These results are presented in compact form in Table I.

A run was then made for a case where the cut-off ratio was greater than one. The case chosen was for a tangential mode number of 5 and a cut-off ratio of 2. This yields a non-dimensional wave number of ka = 12.83. To obtain an exact solution for comparison purposes, both on the surface and in the field, the artifice of a simple source within the body was again employed. Having calculated the distribution of the acoustic potential on the surface of the QCSEE inlet using the normal acoustic velocity distribution is input the normalized average absolute errors of the modulus and phase of the potential were found to be 0.452% and 4.14% respectively.

The computer program that calculates the potential and the acoustic velocity in the field was then used to calculate these acoustic quantities at 38 points in the field surrounding the inlet. These points were placed every 5 degrees from the centerline to 90^{o} from the centerline on two quarter circles centered at the entrance plane of the inlet at distances (radii) of 25a and 100a, where a is the non-dimensionalizing body length (i.e., the inside radius of the inlet at the fan plane). Results were then calculated for two different distributions of the acoustic potential on the surface of the inlet. The first distribution used was the exact one that had been calculated for comparison purposes and the second one was the distribution calculated using the surface code. The exact normal acoustic velocity distribution was used in both cases as it was used as the boundary condition for the surface

solution. The respective computing times for 38 points in the field with 156 points on the surface of the body are 138 sec. and 146 sec.. The difference in computing times is due to the fact that the CDC 70/74 computer that was used has a time sharing system and thus run times vary slightly as the load (number of jobs) on the system changes.

Using the exact distribution of the acoustic potential on the surface of the inlet yielded results with normalized average abslute errors in the modulus and phase of 0.229% and 30.1%. These results are presented in Figs. 1 and 2 in terms of both SPL and PWL in dB along with the exact solution in the field. The equations used for SPL and PWL in dB are presented below in terms of the acoustic potential φ and the outward normal acoustic velocity $\frac{\partial \varphi}{\partial n}$.

$$SPL(dB) = 20 \log_{10} k|\varphi| + 143.6 \tag{2}$$

$$PWL(dB) = 10 \log_{10} k < i\varphi \frac{\partial \varphi}{\partial n} > + 143.3 \tag{3}$$

where <> means time average.

Using the calculated surface solution, the errors were 0.385% and 36.3% respectively and these results are presented in Figs. 3 and 4. Since the error in the phase is so high (compared to the error in the phase in the surface solution) a run was made with more points on the surface of the body using the exact solution on the surface to see if the results would get better as they should. For the case where 230 points were used on the

QCSEE INLET

Deg	SPL (dB)	
	50a	100a
0	−66	−72
5	117	112
10	145	140
15	158	153
20	165	159
25	165	158
30	168	163
35	178	173
40	184	179
45	188	183
50	192	186
55	195	189
60	197	192
65	199	194
70	201	195
75	202	197
80	203	198
85	204	198
90	205	199

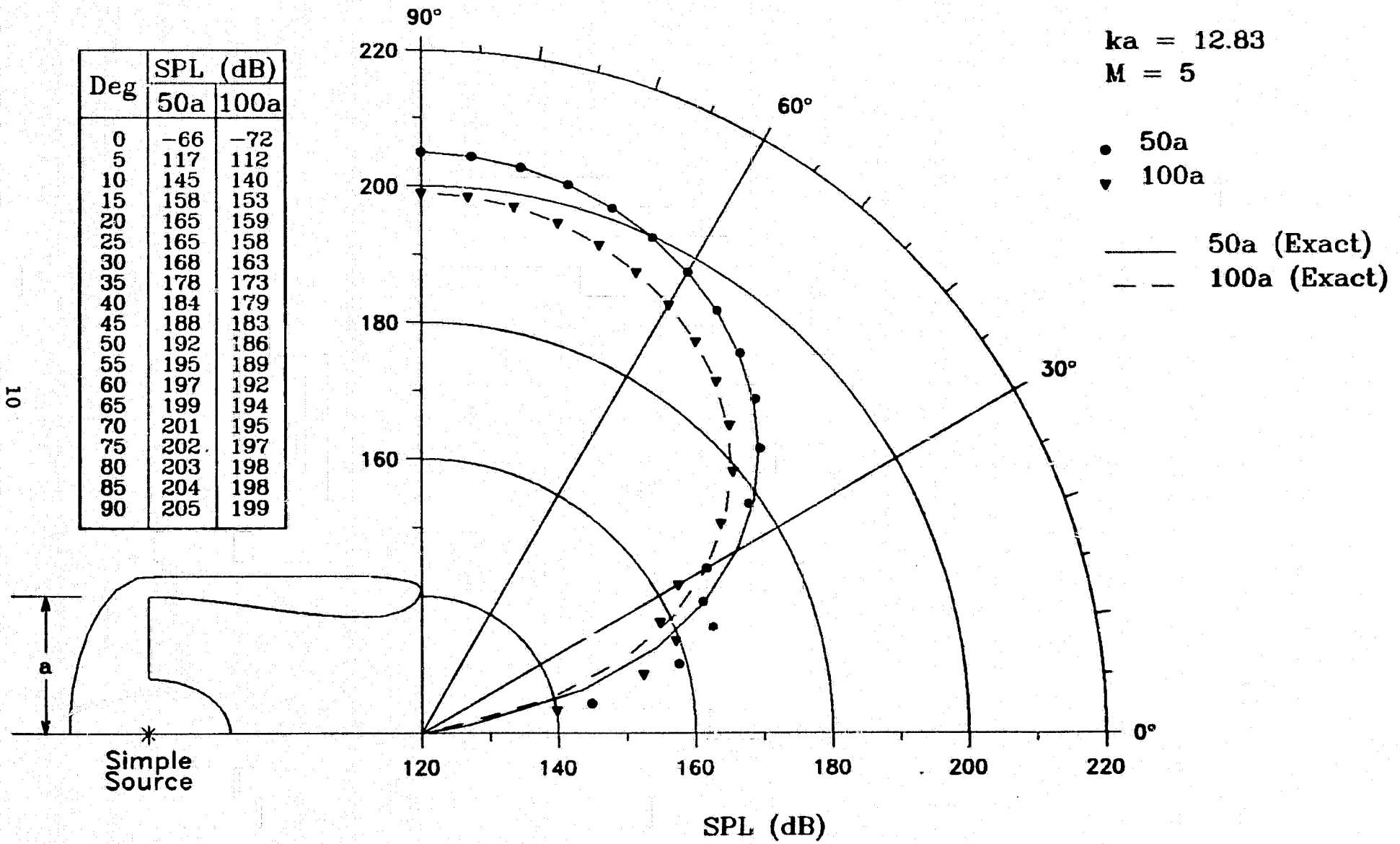

Figure 1. Exact Solution Employed on the Surface at 156 Points, Cut-Off Ratio = 2.

QCSEE INLET

Deg	PWL (dB)	
	50a	100a
0	−66	−73
5	117	112
10	144	139
15	158	153
20	164	159
25	165	158
30	167	162
35	178	173
40	184	179
45	188	183
50	192	186
55	194	189
60	197	191
65	199	193
70	201	195
75	202	196
80	203	197
85	204	198
90	204	198

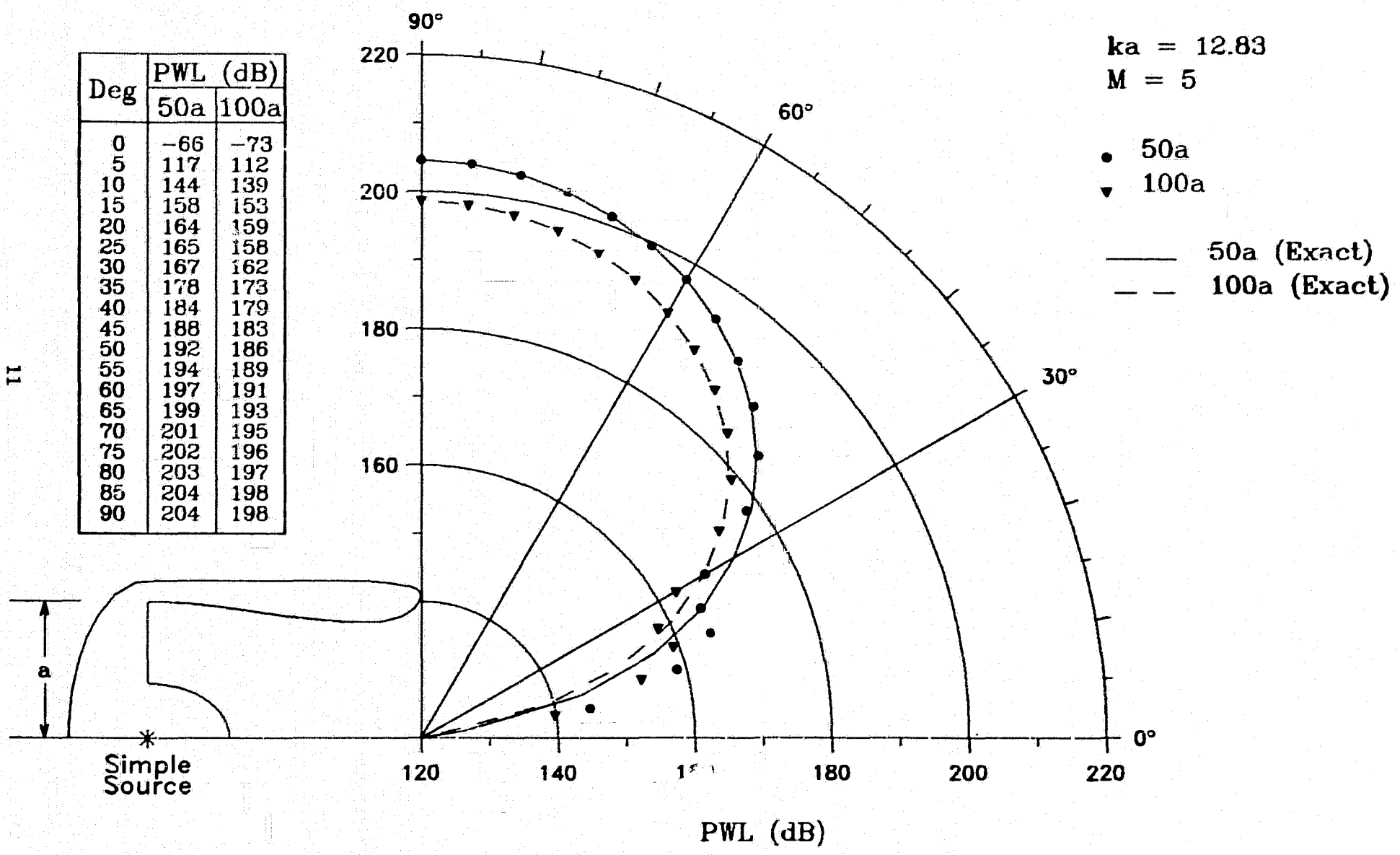

Figure 2. Exact Solution Employed on the Surface at 156 Points. Cut-Off Ratio = 2.

QCSEE INLET

Deg	SPL (dB)	
	50a	100a
0	−67	−72
5	112	107
10	139	133
15	149	144
20	150	145
25	151	143
30	162	158
35	177	172
40	184	179
45	189	183
50	192	187
55	195	189
60	197	192
65	199	194
70	201	196
75	202	197
80	204	198
85	204	198
90	204	198

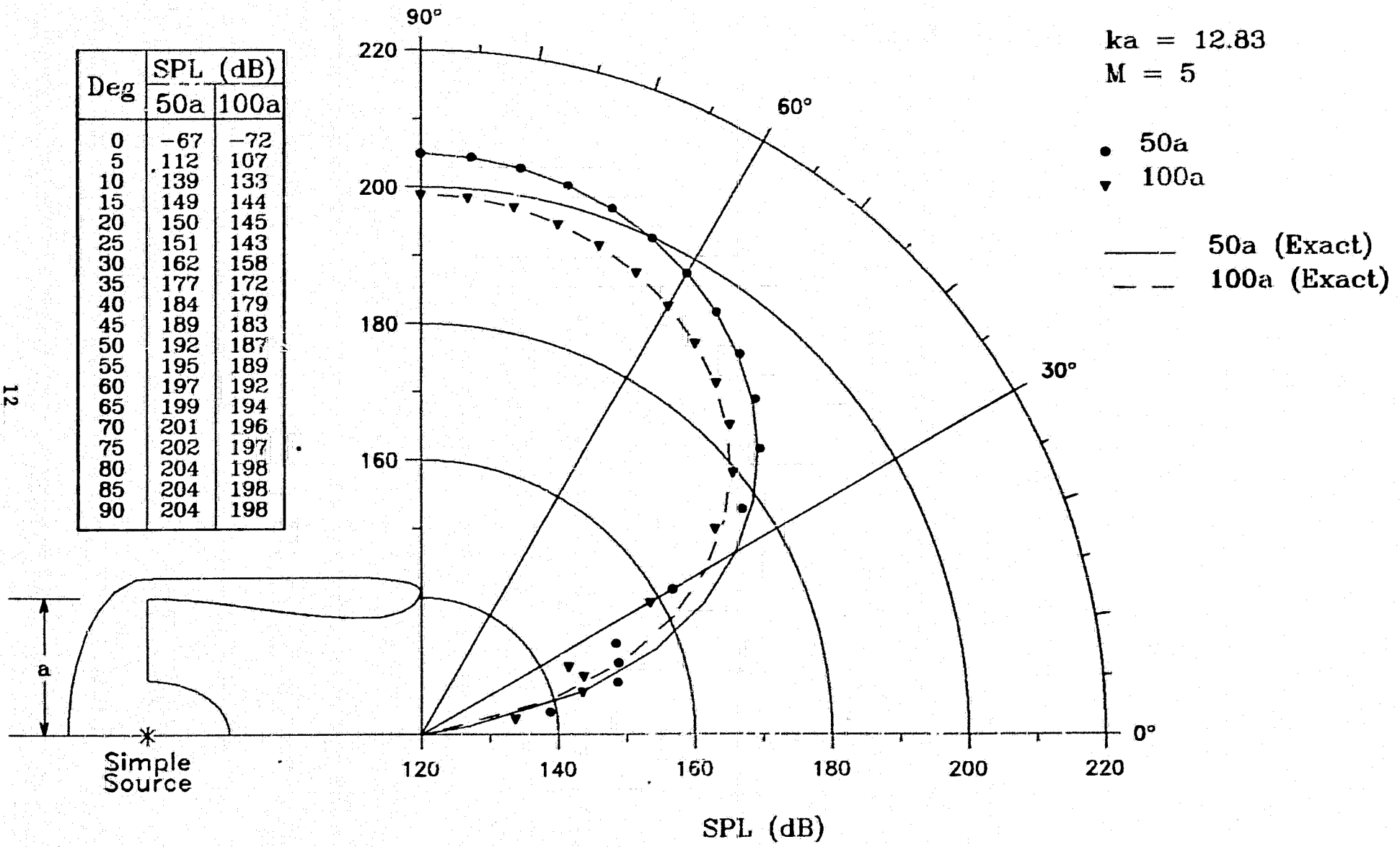

Figure 3. Calculated Solution Employed on the Surface at 156 Points, Cut-Off Ratio = 2.

Deg	PWL (dB)	
	50a	100a
0	−67	−73
5	112	107
10	138	133
15	149	144
20	150	144
25	151	143
30	162	158
35	177	172
40	184	179
45	188	183
50	192	186
55	194	189
60	197	191
65	199	194
70	201	195
75	202	196
80	203	197
85	204	198
90	204	198

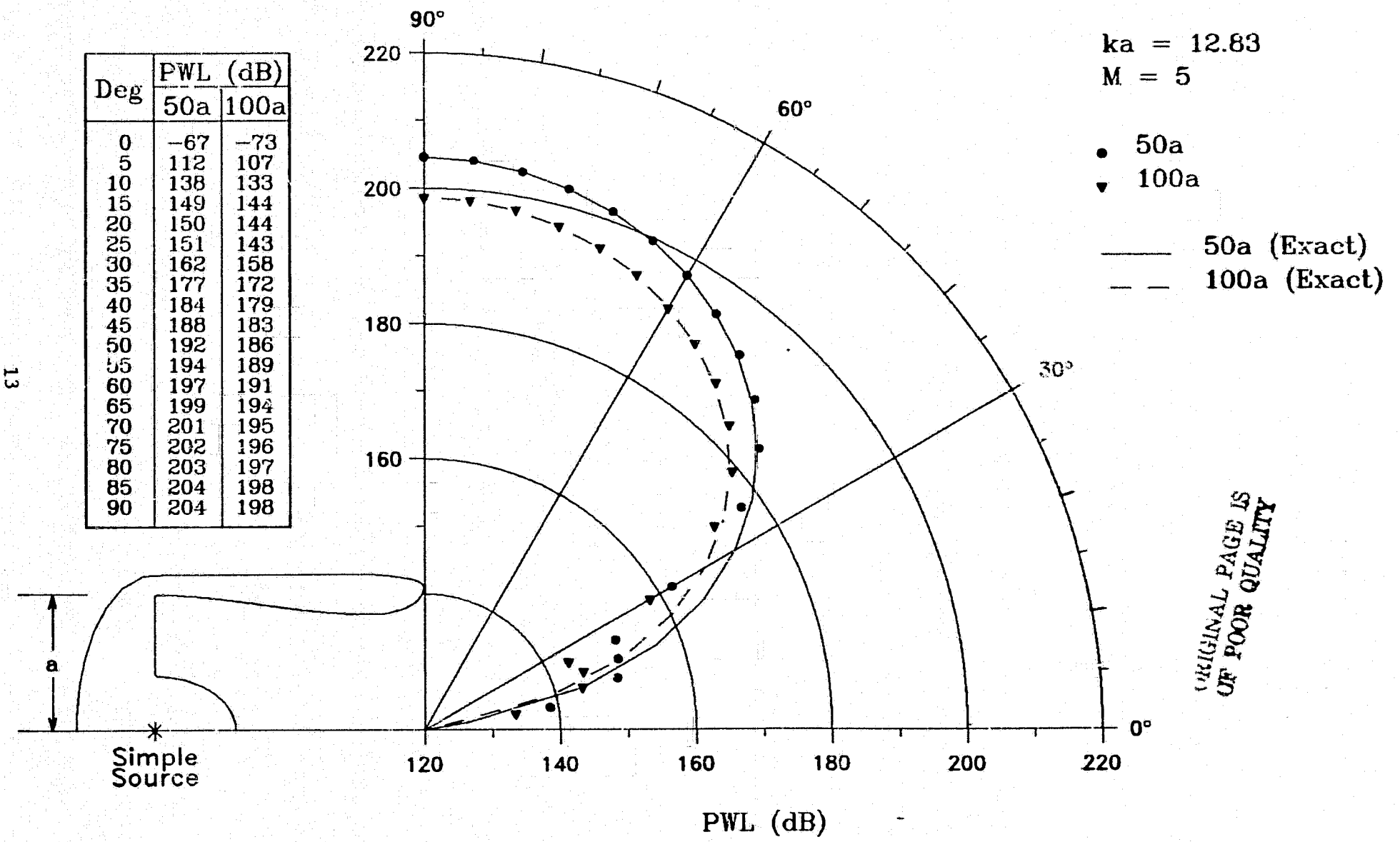

Figure 4. Calculated Solution Employed on the Surface at 156 Points, Cut-Off Ratio = 2.

surface of the inlet with the exact solution specified for both the acoustic potential and normal acoustic velocity the errors in the acoustic potential at 38 points in the field were found to be 0.0127% and 1.18% for the modulus and phase, respectively. These results are presented in Figs. 5 and 6. This shows that the calculated field solutions do converge to the proper values as more points are specified on the surface of the body.

Another set of runs, surface solution and field solution, were then done for a tangential mode number of 2 and a cut-off ratio of 5 so that the non-dimensional wave number is ka = 15.27. The same number of points were used in this case as in the previous one (i.e., 156 points on the body and 38 points in the field) and again the artifice of a simple source within the inlet was employed.

For the surface solution the normalized average absolute errors of the modulus and phase of the acoustic potential was found to be 1.42% and 5.35%, respectively. Since this run is for a relatively low tangential mode number M = 2 the modulus of the acoustic potential on the surface of the body doesn't change much (i.e., it only changes 4 orders of magnitude) so that the average absolute percent errors are a relatively good measure of the error also. For comparison purposes they were computed and found to be 9.87% and 13.7% for the modulus and phase, respectively.

The acoustic potential and the outward normal acoustic velocity were then calculated in the field on the same two quarter circles as before. The normalized average absolute percent errors are found to be 1.27% and 8.59% respectively for the modulus and phase of the acoustic potential. These results are plotted in Figs. 7 and 8 in terms of SPL and PWL in dB as before.

QCSEE INLET

Deg	SPL (dB)	
	50a	100a
0	−66	−72
5	95	90
10	125	121
15	143	138
20	156	151
25	165	160
30	173	167
35	179	174
40	184	179
45	188	183
50	192	186
55	195	189
60	197	192
65	199	194
70	201	195
75	202	197
80	203	198
85	204	198
90	205	199

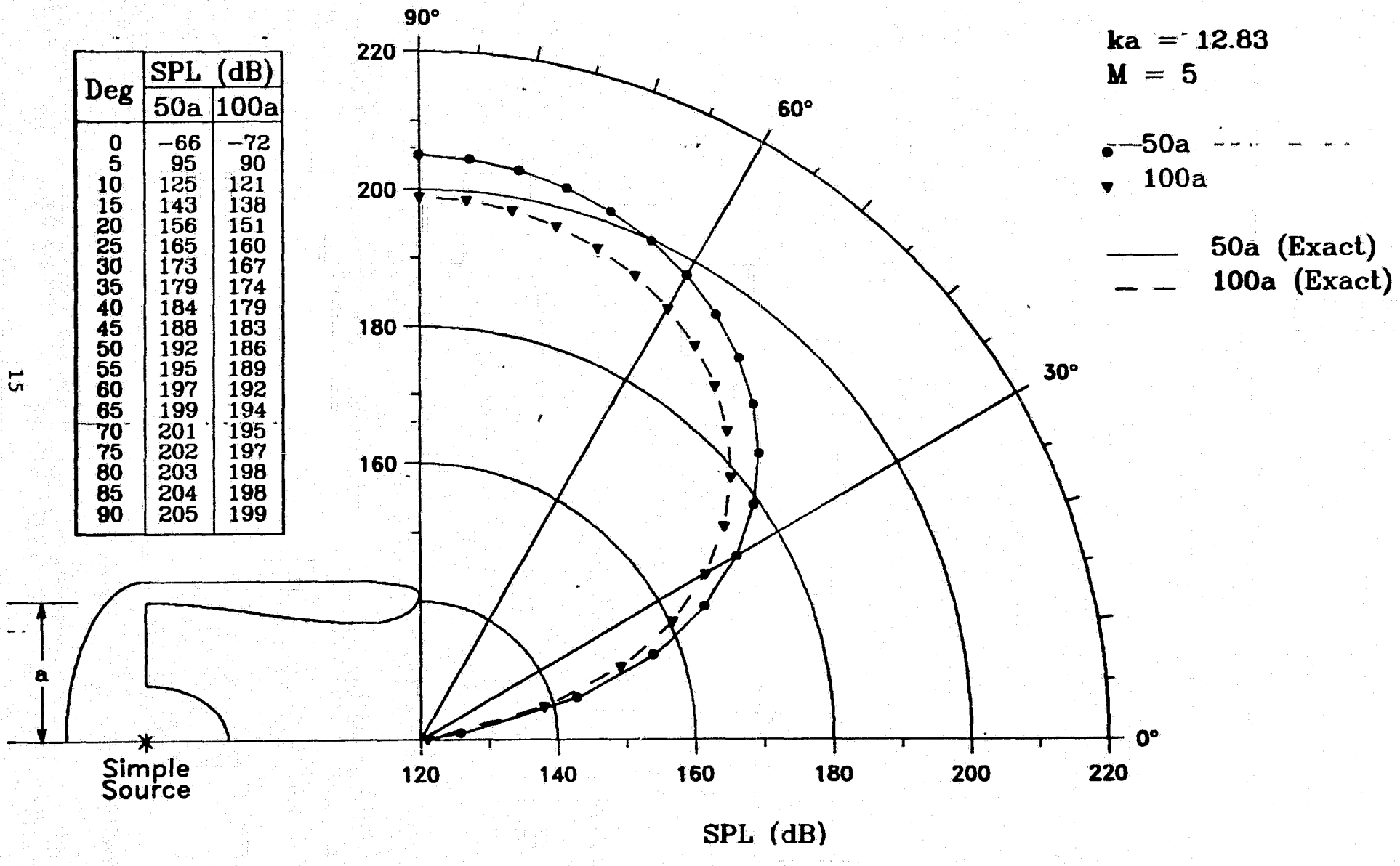

Figure 5. Exact Solution Employed on the Surface at 230 Points, Cut-Off Ratio = 2.

QCSEE INLET

Deg	PWL (dB)	
	50a	100a
0	−66	−72
5	95	90
10	125	120
15	143	138
20	155	150
25	165	160
30	172	167
35	178	173
40	183	178
45	188	182
50	191	186
55	194	189
60	197	191
65	199	194
70	201	195
75	202	196
80	203	197
85	204	198
90	204	198

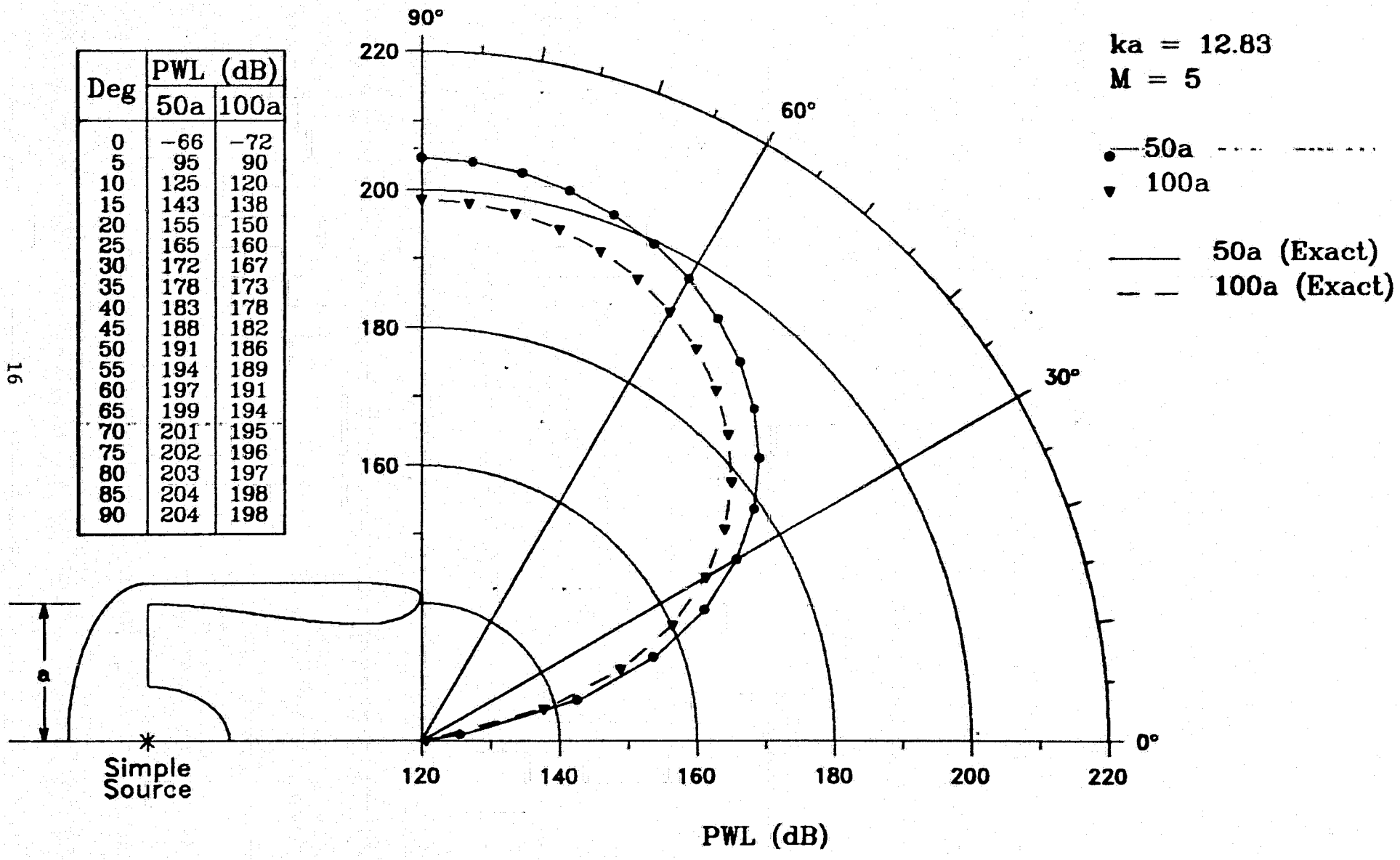

Figure 6. Exact Solution Employed on the Surface at 230 Points, Cut-Off Ratio = 2.

QCSEE INLET

Deg	SPL (dB)	
	25a	100a
0	0	0
5	104	93
10	112	100
15	113	101
20	116	105
25	120	109
30	121	110
35	122	111
40	125	114
45	127	116
50	128	117
55	129	118
60	131	120
65	132	120
70	132	121
75	133	122
80	134	122
85	134	122
90	134	122

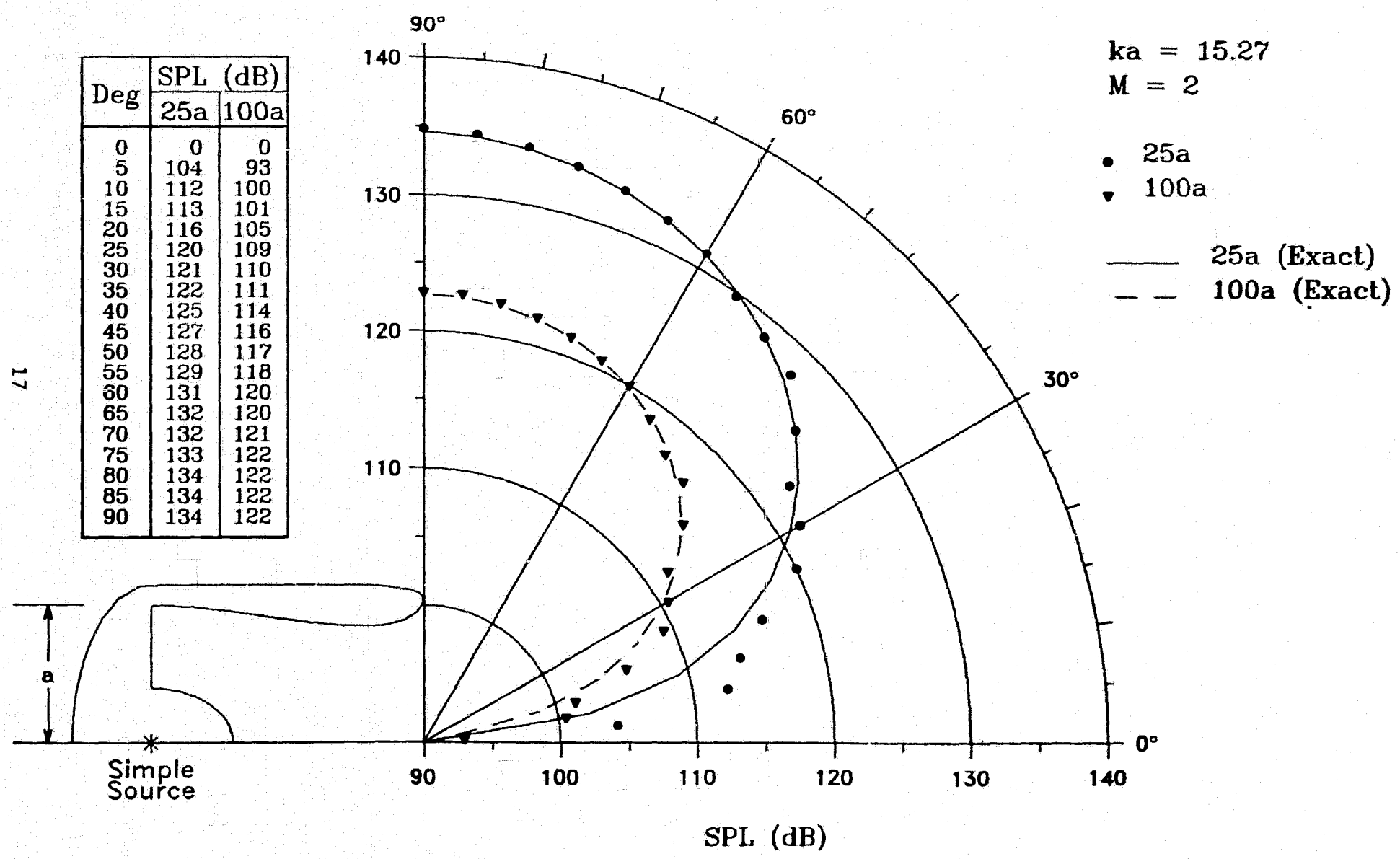

Figure 7. 156 Points on the Surface, Cut-Off Ratio = 5.

QCSEE INLET

Deg	PWL (dB)	
	25a	100a
0	0	0
5	103	92
10	112	100
15	113	101
20	116	105
25	119	109
30	121	110
35	122	111
40	125	114
45	127	116
50	128	117
55	129	118
60	130	119
65	131	120
70	132	121
75	133	121
80	133	122
85	134	122
90	134	122

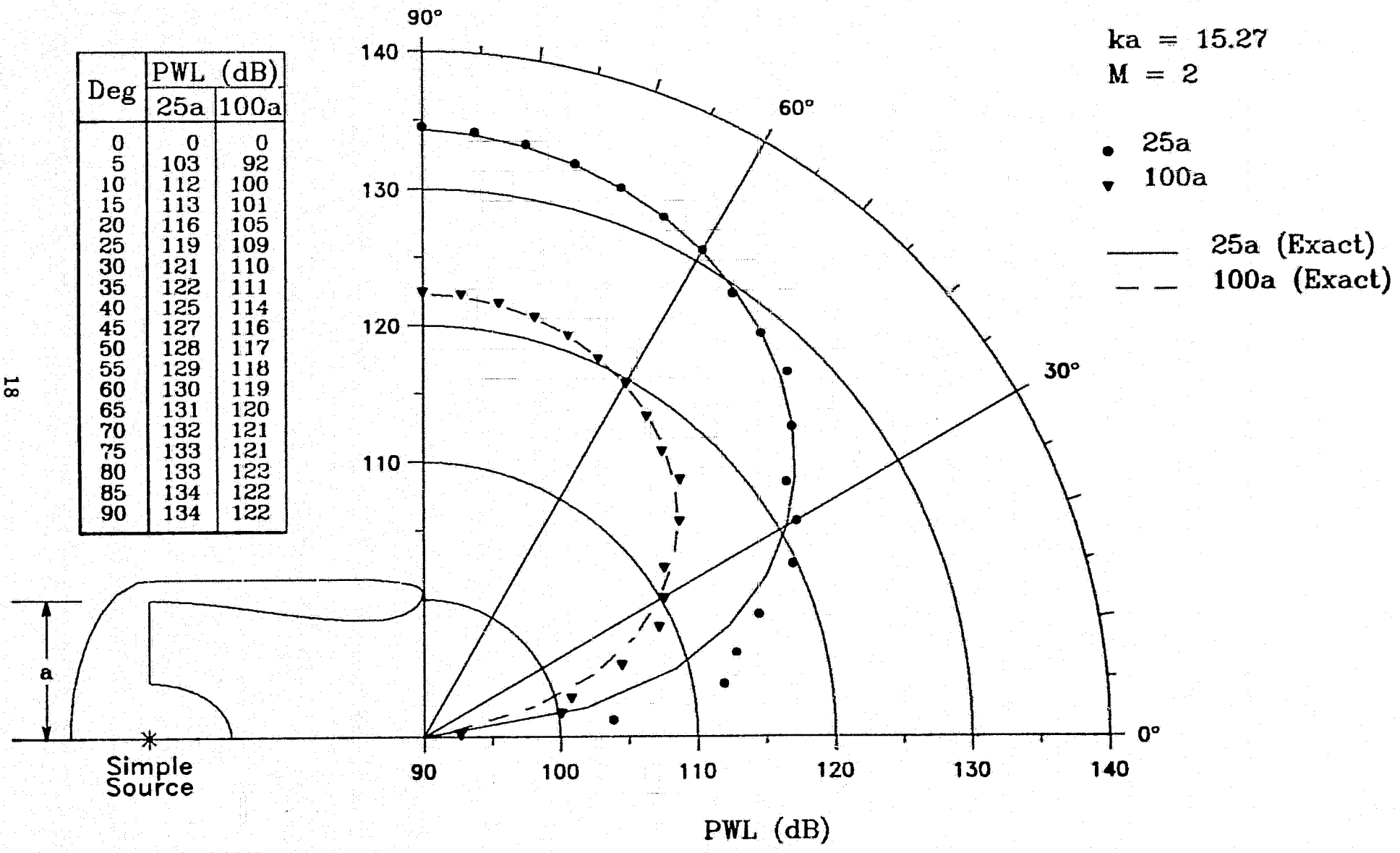

Figure 8. 156 Points on the Surface, Cut-Off Ratio = 5.

Also, a summary of the results for the two cases where 156 points were used on the surface of the body are presented in Table II.

The final two runs were made for a case that will be run for the NASA Lewis JT15D bellmouth inlet. This particular case was chosen as it requires the highest non-dimensional wave number and therefore should represent the worst case (i.e., the case with the most error). For this case a tangential mode number of M = 13 and a cut-off ratio of 1.30 were used which translates into a non-dimensional wave number of ka = 19.41. On both of the following runs 181 points were specified on the surface of the QCSEE inlet.

For the first run of the set the artifice of a simple source was again used so that an exact solution would be known and the error could be calculated. The normalized average absolute error in the modulus and phase of the acoustic potential were found to be 0.105% and 24.0% on the surface and 0.111% and 38.2% in the field. The results in SPL and PWL in dB are presented in Figs. 9 and 10. In evaluating these results, it should be pointed out that considering the range of dB values covered by the solution, the errors in dB are relatively small.

For the final run, the simple source was not used; instead, the acoustic velocity was specified for the 13th tangential mode at the fan plane and the rest of the body was specified as having a hard wall (i.e., $\frac{\partial \Phi}{\partial n} = 0$). First, the surface distrubution of the acoustic potential was calculated (1131 sec.) and then the values of the acoustic potential and outward normal acoustic velocity were calculated at 38 points in the field as before (142 sec.). Finally the results were plotted as before (See Figs. 11 and 12.) except

QCSEE INLET

Deg	SPL (dB)	
	25a	100a
0	246	234
5	253	249
10	304	295
15	345	336
20	371	360
25	385	370
30	398	385
35	409	396
40	426	418
45	435	426
50	439	433
55	451	443
60	457	449
65	463	455
70	468	459
75	472	462
80	475	464
85	477	466
90	478	467

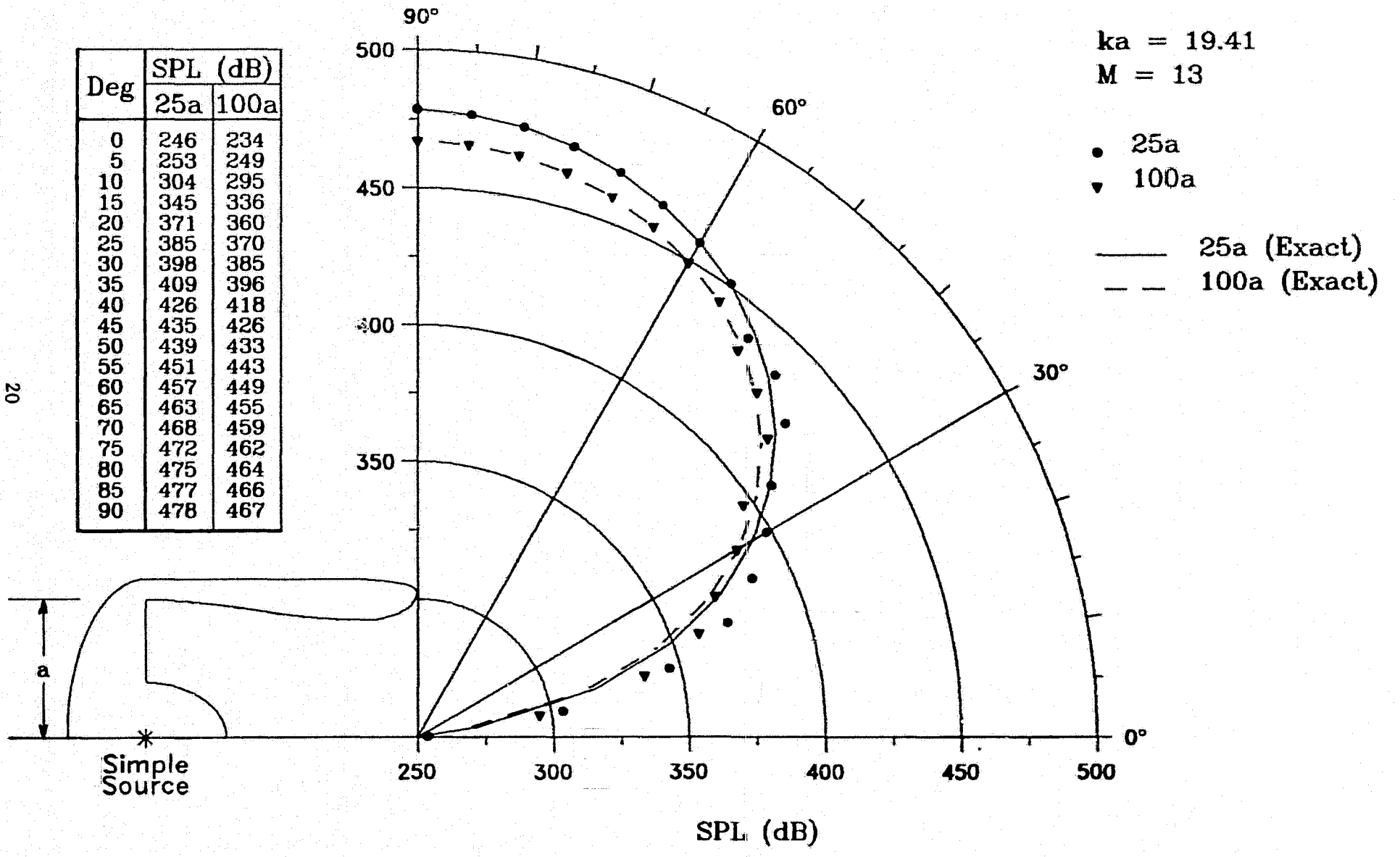

Figure 9. Simple Source Case, 181 Points on the Surface, Cut-Off Ratio = 1.3.

QCSEE INLET

Deg	PWL (dB)	
	25a	100a
0	245	234
5	253	248
10	303	295
15	345	336
20	371	359
25	385	370
30	397	385
35	408	396
40	426	417
45	435	426
50	438	433
55	450	443
60	457	449
65	463	454
70	468	458
75	472	462
80	475	464
85	477	466
90	478	466

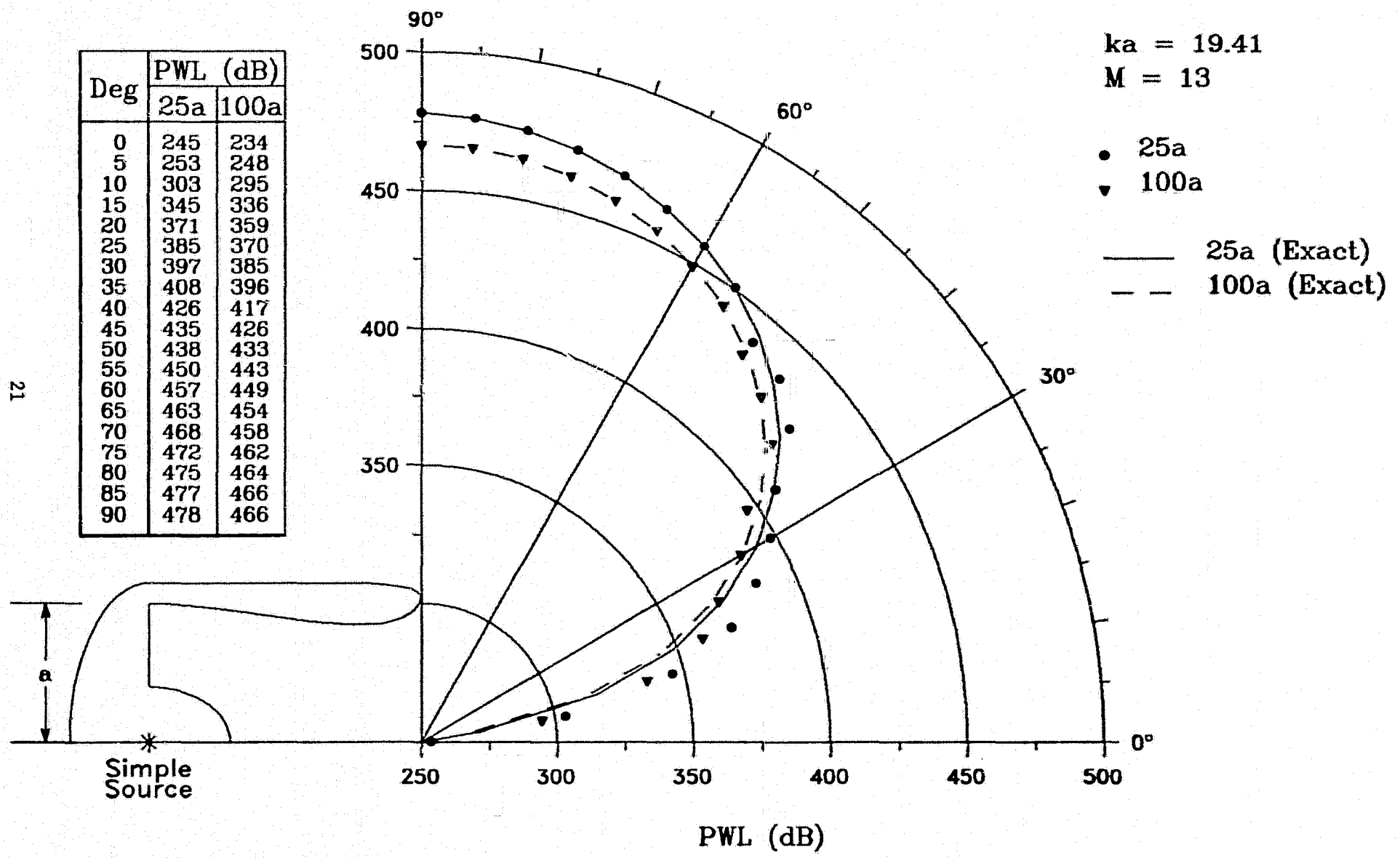

Figure 10. Simple Source Case, 181 Points on the Surface, Cut-Off Ratio = 1.3.

QCSEE INLET

Deg	SPL (dB)	
	25a	100a
0	0	0
5	−87	−99
10	−11	−23
15	31	19
20	59	47
25	80	68
30	95	83
35	105	93
40	112	100
45	116	105
50	119	107
55	119	107
60	120	108
65	119	107
70	117	105
75	115	103
80	113	101
85	111	99
90	110	97

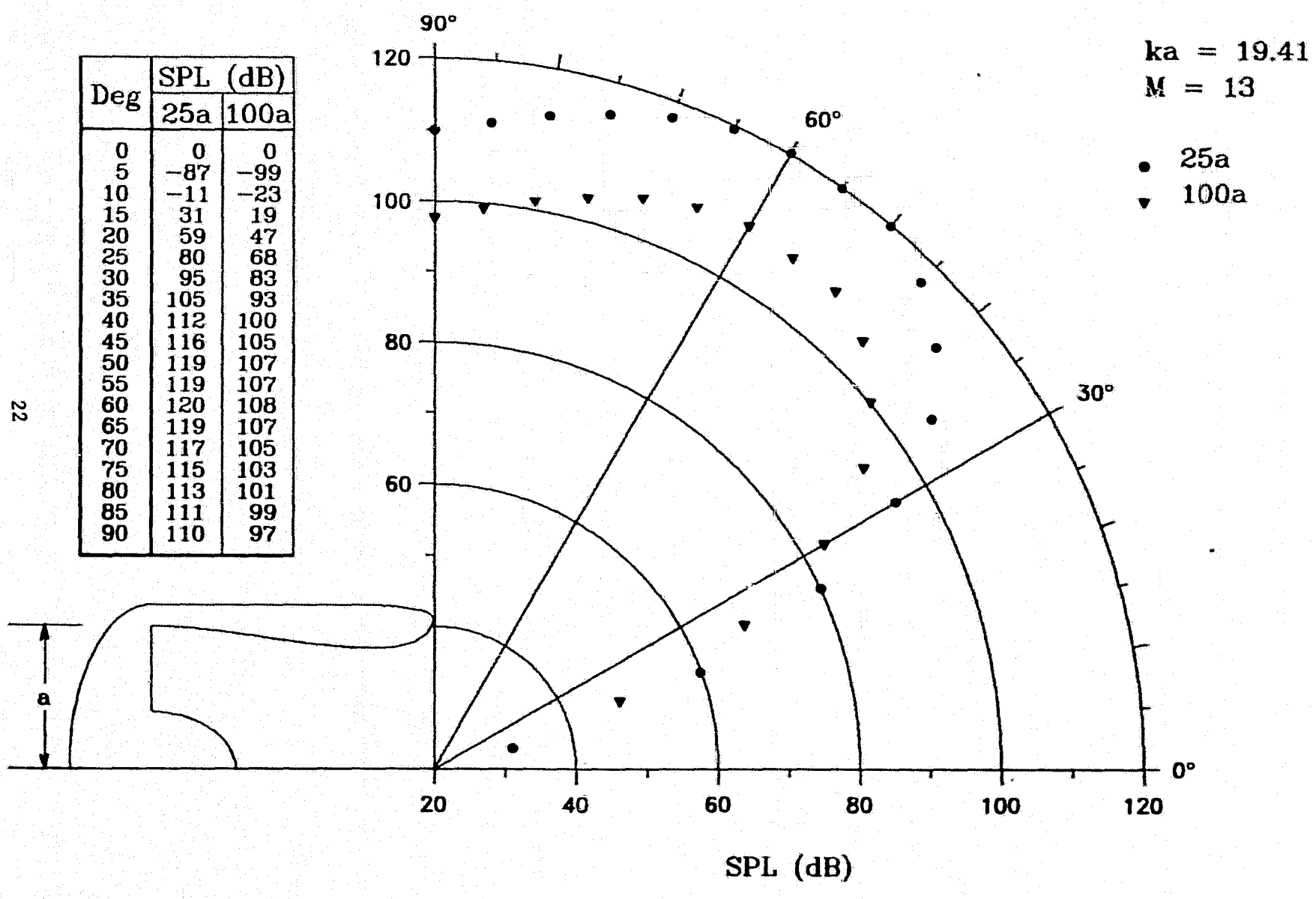

Figure 11. Modal Source Distribution at the Fan Plane, 181 Points on the Surface, Cut-Off Ratio = 1.3.

QCSEE INLET

Deg	PWL (dB)	
	25a	100a
0	0	0
5	−87	−99
10	−11	−23
15	31	19
20	59	47
25	79	67
30	94	83
35	105	93
40	111	99
45	116	104
50	119	107
55	119	107
60	119	108
65	119	106
70	117	105
75	115	102
80	113	100
85	111	99
90	109	97

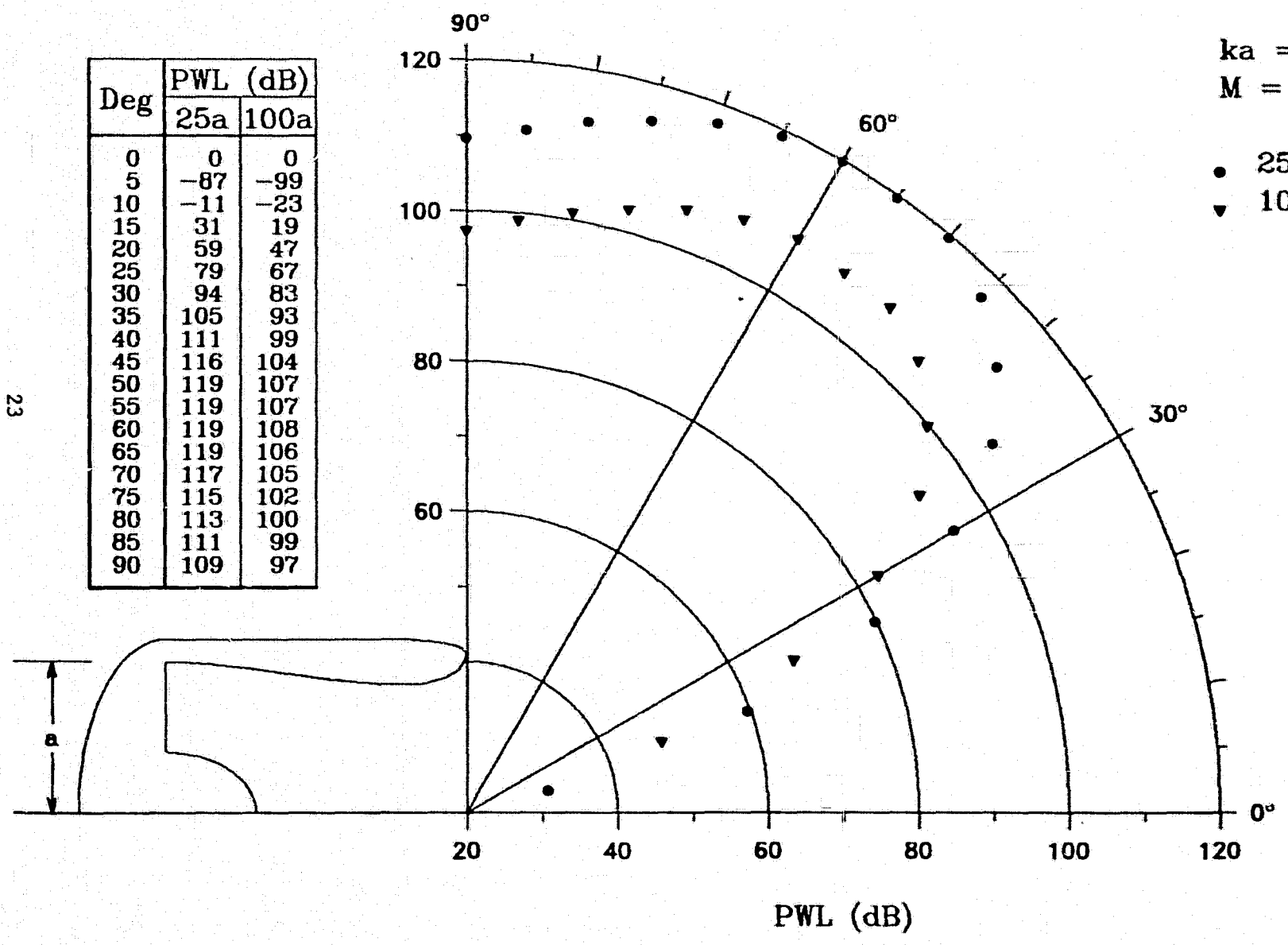

Figure 12. Modal Source Distribution at the Fan Plane, 181 Points on the Surface, Cut-Off Ratio = 1.3.

that for this case no exact solution was available. It should be noted here that a computer program has been developed to calculate the normal acoustic velocity distribution at the fan plane for any mode (tangential and radial).

SUMMARY

During the first half of this contract period the basic computer programs have been made much more efficient and accurate. Furthermore, they have been upgraded so that they can handle many more points on the surface of the body thus significantly extending their range of applicability. Also, new computer programs have been developed to help generate the required input data for these programs. This data consists of the body geometry and the input modal distribution at the fan plane. Another program has been developed which can accurately calculate the modal cut-off wave numbers for any tangential and radial mode. Finally, a computer program was developed that is capable of plotting the calculated data in the field in terms of SPL and PWL in dB (See Figs. 1-12.).

Various results are calculated for the NASA Lewis QCSEE inlet as part of the test program for the "new", upgraded computer codes. Tangential mode numbers of up to 13 were used with corresponding non-dimensional wave numbers over 19. The artifice of a simple source solution was employed for most of the computer test cases so that error estimates could be calculated. Large improvements in both accuracy and computing time required for the "new" computer codes when compared to the "old" computer codes were found.

Table I

Run	Computing Time sec.	Normalized Average Absolute Error (Potential)	
		Modulus %	Phase %
Bench Mark 105 points	867	0.139	8.75
Improved Computer Code 105 points	309	0.0999	3.10
156 points	791	0.0679	2.59

Various computer runs for the simple source case where M = 10 and ka = 10.0 for the QCSEE inlet.

Table II

Run	Normalized Average Absolute Error (Potential)			
	Surface		Field	
	Modulus %	Phase %	Modulus %	Phase %
Cut-Off Ratio 2 M = 5 ka = 12.83	0.452	4.14	0.385	36.3
Cut-Off Ratio 5 M= 2 ka = 15.27	1.42	5.35	1.27	8.59

Computer runs for the simple source cases with 156 points on the surface of the QCSEE Inlet.

Appendix A

Prediction of the Sound Field Radiated from Axisymmetric Surfaces (Ref.3)

Prediction of the sound field radiated from axisymmetric surfaces

W. L. Meyer and W. A. Bell

School of Aerospace Engineering, Georgia Institute of Technology, Atlanta, Georgia 30332

M. P. Stallybrass

School of Mathematics, Georgia Institute of Technology, Atlanta, Georgia 30332

B. T. Zinn

School of Aerospace Engineering, Georgia Institute of Technology, Atlanta, Georgia 30332
(Received 19 March 1978; revised 10 September 1978)

A general analytical method for determining the radiated sound fields from axisymmetric surfaces of arbitrary cross section with general boundary conditions is developed. The method is based on an integral representation for the external solutions of the Helmholtz equation. An integral equation is developed governing the surface potential distribution which gives unique solutions at all wavenumbers. The axisymmetric formulation of the problem reduces its solution to the numerical evaluation of line integrals by Gaussian quadrature. The applicability of the solution approach for both a sphere and finite cylinder is demontrated by comparing the numerical results with exact analytical solutions for both discontinuous and continuous boundary conditions. The method is then applied to a jet-engine-inlet configuration and the computed results are in good agreement with exact values.

PACS numbers: 43.20.Rz, 43.20.Tb

INTRODUCTION

To reduce the noise radiated to the community from turbofan inlets, the effects of sound suppression material in the inlet and the spatial distribution of the sound source on the radiated sound levels and patterns must be determined. Analytical techniques for predicting these effects must be capable of dealing with general axisymmetric geometries and complicated boundary conditions which are encountered in multiply lined inlets. For instance, in a typical inlet the compressor-fan combination represents a noise source with a nonuniform spatial excitation pattern. Thus, the analytical method should be capable of taking into account sound sources of general spatial distribution. Also, inlets may contain multiple acoustic liners to reduce the radiated sound power, and admittance boundary conditions are commonly used to account for the absorption characteristics of the liner. Therefore, the analytical method must be capable of dealing with spatially varying surface admittances. Finally, the method should be capable of predicting the characteristics of the radiated sound field in an infinite domain. Keeping these requirements in mind, the work presented in this paper describes the results of an investigation which has been concerned with the analytical determination of radiated sound fields from axisymmetric surfaces of arbitrary cross section and with general boundary conditions.

The method used in this investigation is based on an integral form of the solutions of the Helmholtz equation.[1-6] With this formulation the acoustic potential anywhere external to the surface can be found once the distribution on the surface is known. Thus, to determine the radiated sound field the problem reduces to the determination of the distribution of the acoustic potential on the two-dimensional surface of the geometry under consideration instead of solving the Helmholtz equation in the surrounding infinite three-dimensional domain.

It has been previously shown[1-5] that when applied to exterior sound radiation problems the classical techniques fail to produce unique solutions at frequencies corresponding to certain interior eigenvalues of the geometries under consideration. Unless special precautions are taken, straightforward numerical solution of the integral equation produces large errors at frequencies close to these eigenvalues. For the general geometries of interest in this study, these eigenfrequencies are not known *a priori*. Therefore, the frequencies about which large numerical errors can occur cannot be easily avoided. A critical review of available analytical techniques for avoiding these errors is provided by Burton in Ref. 1. In a search for an appropriate technique for use in the present study of inlets, the authors programmed each of these methods for a sphere and obtained numerical results for the surface and radiated sound fields. This study showed that the method of Burton and Miller[4] was the most straightforward to implement. However, an interpretation of a strongly singular integral, given in the analysis in Ref. 5 by Meyer *et al.*, was necessary for the equations to be amenable to numerical solution. Basically the method proposed by Burton and Miller involves a reformulation of the integral equation for the acoustic potential, and the solutions obtained are valid at all frequencies. It also yields the most consistently accurate results for a given number of points at which the acoustic potential is numerically evaluated on the surface. Therefore, the method based on the analysis in Ref. 5 has been chosen for this investigation.

The resulting integral equation for the surface acoustic potential is solved numerically and, for axisymmetric geometries, the equation reduces to the evaluation

 0001-4966/79/030631-08$00.80

of line integrals. Thus, the axisymmetric case can be reduced to an equivalent one-dimensional problem. Having discretized the integral equation, the resulting system of algebraic equations is solved using complex Gauss–Jordan elimination. Since the coefficient matrix involves the free-space Green's function, which becomes singular as two points on the surface approach one another, numerical techniques are presented which can deal with these singularities and yield accurate results. Gaussian integration is used to increase the accuracy of the solution without significant penalties in computer storage and time requirements. The applicability of the integral formulation and the accuracy of the numerical techniques are demonstrated by computing the surface and farfield distribution of the acoustic potential on both a sphere and a finite cylinder. The numerical results are compared with known exact solutions generated by the separation of variables technique. Surfaces with spatially varying forcing functions and admittances are considered, for different tangential modes, to evaluate the capability of the integral approach to handle boundary conditions of a general nature. With the sphere, agreement between computed and exact results is to three significant figures. For the cylinder agreement is to two significant figures. The effect on the accuracy of discontinuous boundary conditions involving nonzero admittances over the surface and of the corners encountered in the cylindrical configuration are also presented. Finally, the numerical results for an inlet configuration are compared with exact solutions and agreement is to within 10%.

I. THEORETICAL CONSIDERATIONS

In this section the general three-dimensional integral representation of the solutions of the Helmholtz equation is developed for application to radiation problems. This particular formulation yields unique solutions at all frequencies and does not have strong singularities which are difficult to handle numerically. The general integral equation is then specialized for axisymmetric geometries. A more detailed development is presented in Ref. 5.

A. General formulation

Beginning with the three-dimensional Helmholtz equation which governs the spatial dependence of the acoustic field for harmonic oscillations

$$\nabla^2\varphi + k^2\varphi = 0 \ , \tag{1}$$

where φ is the acoustic potential and k is the wavenumber; the standard integral representation of the exterior potential is found to be[1,6]

$$\int_S\int\left(\varphi(Q)\,\frac{\partial G(P,Q)}{\partial n_q} - G(P,Q)\,\frac{\partial\varphi(Q)}{\partial n_q}\right)dS_q = 4\pi\varphi(P) \ , \tag{2}$$

where the term $\partial/\partial n_q$ represents an outward normal derivative with respect to the body S as shown in Fig. 1, that is

$$\frac{\partial\varphi(Q)}{\partial n_q} = \nabla_q\varphi(Q)\cdot\mathbf{n}_q \ . \tag{3}$$

Also, $G(P, Q)$ is a fundamental three-dimensional solution of the Helmholtz equation and is taken to be the free-space Green's function for a point source[6] defined as

$$G(P,Q) = \exp[ikr(P,Q)]/r(P,Q) \ . \tag{4}$$

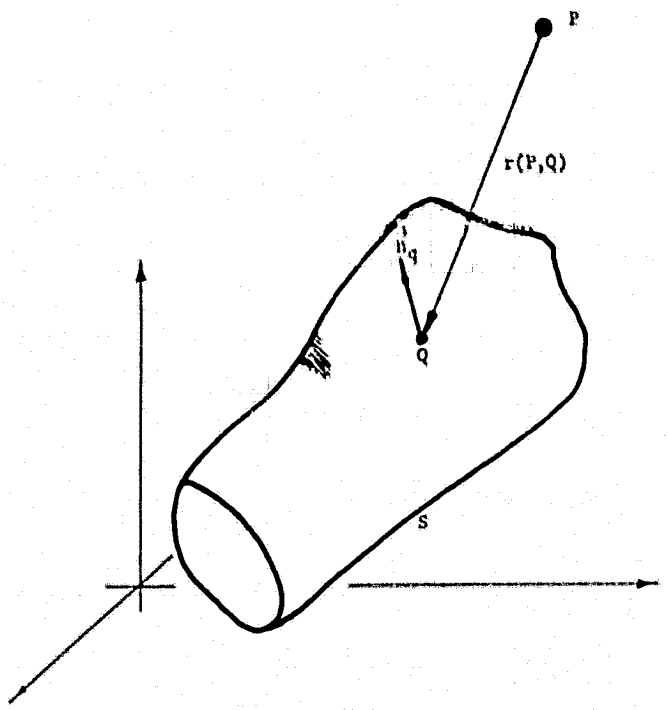

FIG. 1. Geometrical properties of the general acoustic radiation problem.

From Eq. (2), if the acoustic potential and the normal acoustic velocity $\partial\varphi(Q)/\partial n_q$ are known at each point on the surface of the body, then the acoustic potential may be calculated anywhere in the exterior domain.

To solve for the surface potential, the point P is moved to the surface of the body, and Eq. (2) then becomes

$$\int_S\int\left(\varphi(Q)\,\frac{\partial G(P,Q)}{\partial n_q} - G(P,Q)\,\frac{\partial\varphi(Q)}{\partial n_q}\right)dS_q = 2\pi\varphi(P) \ . \tag{5}$$

For the inhomogeneous Robin boundary condition employed in this study, a relation between $\partial\varphi(Q)/\partial n_q$ and $\varphi(Q)$ exists and is given by

$$\frac{\partial\varphi(Q)}{\partial n_q} - Y(Q)\,\varphi(Q) = A(Q) \ , \tag{6}$$

so that Eq. (5) can be written in terms of the potential only, that is,

$$\int_S\int\varphi(Q)\,\frac{\partial G(P,Q)}{\partial n_q}\,dS_q - \int_S\int\varphi(Q)\,G(P,Q)\,Y(Q)\,dS_q = 2\pi\varphi(P) + \int_S\int A(Q)\,G(P,Q)\,dS_q \ . \tag{7}$$

If the acoustic velocity $A(Q)$ and the admittance $Y(Q)$ are specified at each point on the surface of the body, then the acoustic potential may be calculated at each point using Eq. (7).

As mentioned earlier this equation does not yield unique solutions when the wavenumber k is an internal

eigenvalue associated with the problem under consideration. Since these eigenvalues are not known *a priori* for general bodies, the formulation cannot be relied upon to give consistently good results. There are a number of papers in the literature[2-4] dealing with this problem, and the relative merits and shortcomings of the methods employed are discussed in detail in Ref. 1.

An attractive approach from an analytical point of view is provided by Burton and Miller,[4] who have suggested the use of the following identity to derive an alternative integral equation for the acoustic potential at the surface:

$$2\pi \frac{\partial\varphi(P)}{\partial n_p} = \int_S\int \left(\varphi(Q) \frac{\partial^2 G(P,Q)}{\partial n_p \partial n_q} - \frac{\partial G(P,Q)}{\partial n_p} \frac{\partial\varphi(Q)}{\partial n_q}\right) dS_q \ . \tag{8}$$

This equation can now be solved for $\varphi(P)$ by using Eq. (6) to relate the normal acoustic velocity and the potential at the surface. However this integral equation has its own set of associated eigenvalues at which unique solutions cannot be obtained. To circumvent the problem associated with the solution of the integral equations derived from Eqs. (5) and (8), Burton and Miller suggested the solution of the following linear combination of these equations:

$$\int_S\int \left(\varphi(Q) \frac{\partial G(P,Q)}{\partial n_q} - G(P,Q) \frac{\partial\varphi(Q)}{\partial n_q}\right) dS_q + \alpha \int_S\int \left(\varphi(Q) \frac{\partial^2 G(P,Q)}{\partial n_p \partial n_q} - \frac{\partial G(P,Q)}{\partial n_p} \frac{\partial\varphi(Q)}{\partial n_q}\right) dS_q$$
$$= 2\pi\left(\varphi(P) + \alpha \frac{\partial\varphi(P)}{\partial n_p}\right) , \tag{9}$$

where $\partial\varphi/\partial n$ and φ are related by Eq. (6). Equation (9) will yield unique solutions if the complex coupling constant is properly chosen. It is shown that α must meet the following restrictions to guarantee that Eq. (9) yields unique solutions[7]:

$$\begin{aligned} &\mathrm{Im}(\alpha) \neq 0 \ , \quad k \text{ real or imaginary} \ , \\ &\mathrm{Im}(\alpha) = 0 \ , \quad k \text{ complex} \ . \end{aligned} \tag{10}$$

A problem arises in the numerical solution of Eq. (9) as the third term on the left hand side is strongly singular in its present form as the point Q approaches the point P on the surface of the body. The authors of this paper have shown that this difficulty can be overcome by a proper interpretation of this singular term.[5] Employing a vector transformation[8] and taking the Cauchy Principle Value, Eq. (9) is shown to be equivalent to

$$\int_S\int \left(\varphi(Q) \frac{\partial G(P,Q)}{\partial n_q} - G(P,Q) \frac{\partial\varphi(Q)}{\partial n_q}\right) dS_q + \alpha \int_S\int [\varphi(Q) - \varphi(P)] \frac{\partial^2 G(P,Q)}{\partial n_p \partial n_q} dS_q$$
$$- \alpha\varphi(P) \int_S\int (n_p \cdot n_q)(ik)^2 G(P,Q)\, dS_q - \alpha \int_S\int \frac{\partial G(P,Q)}{\partial n_q} \frac{\partial\varphi(Q)}{\partial n_q} dS_q = 2\pi\left(\varphi(P) + \alpha \frac{\partial\varphi(P)}{\partial n_p}\right) . \tag{11}$$

All of the terms in Eq. (11) are now well defined; however, all integrands are oscillatory and singular so that care must be taken in their numerical approximation.

B. Axisymmetric formulation

When dealing with a body of revolution as shown in Fig. 2 an axisymmetric formulation of the problem is advantageous.[10] This being the case an element of area dS_q becomes $\rho\, ds\, d\theta$, where s is the distance along the perimeter of the surface in the $\rho - z$ plane. Assuming an acoustic velocity distribution of the form

$$\frac{\partial\varphi}{\partial n} = v(s)\cos(m\theta) \ , \tag{12}$$

and describing the s dependence of the potential function by

$$\Phi(s) \equiv \varphi/\cos(m\theta) \ , \tag{13}$$

and letting $\theta_p = 0$ (so that $\cos\theta_p = 1$) Eq. (11) becomes:

$$\int_S\int \Phi(s_q) \frac{\partial G(P,Q)}{\partial n_q} \cos(m\theta_q)\, dS_q - \alpha\, \Phi(s_p) \int_S\int G(P,Q)\,(ik)^2 (n_p \cdot n_q)\, dS_q$$
$$+ \alpha \int_S\int [\Phi(s_q)\cos(m\theta_q) - \Phi(s_p)] \frac{\partial^2 G(P,Q)}{\partial n_p \partial n_q} dS_q - \int_S\int v(s_q)\, G(P,Q)\cos(m\theta_q)\, dS_q$$
$$- \alpha \int_S\int v(s_q) \frac{\partial G(P,Q)}{\partial n_p} \cos(m\theta_q)\, dS_q = 2\pi[\Phi(s_p) + \alpha v(s_p)] \ . \tag{14}$$

Now, three sets of functions are defined:

Influence functions:

$$I_1(r_{pq}) = 2\int_0^{\pi} G(P,Q)\cos(m\theta_q)\, d\theta_q \ ,$$

$$I_2(r_{pq}) = 2\alpha \int_0^{\pi} \frac{\partial G(P,Q)}{\partial n_p} \cos(m\theta_q)\, d\theta_q \ ; \tag{15}$$

Kernel functions:

$$K_1(r_{p_\theta}) = 2\int_0^{\pi} \frac{\partial G(P,Q)}{\partial n_\theta}\cos(m\theta_\theta)\,d\theta_\theta \ ,$$
$$K_2(r_{p_\theta}) = 2\alpha\int_0^{\pi} \frac{\partial^2 G(P,Q)}{\partial n_p\,\partial n_\theta}\cos(m\theta_\theta)\,d\theta_\theta, \ \theta_\theta \neq \theta_p \ ; \tag{16}$$

Forcing functions:

$$F_1(r_{p_\theta}) = 2\alpha\int_0^{\pi} G(P,Q)\,(ik)^2(n_p \cdot n_\theta)\,d\theta_\theta \ ,$$
$$F_2(r_{p_\theta}) = 2\alpha\int_0^{\pi} \frac{\partial^2 G(P,Q)}{\partial n_p\,\partial n_\theta}\,d\theta_\theta \ , \ \theta_\theta \neq \theta_p \ , \tag{17}$$

where r_{p_θ} is the distance between points P and Q and n_p and n_θ are the outward normals to the surface at points P and Q, respectively. In evaluating K_2 and F_2, the point at which $\theta_p = \theta_\theta$ is excluded from the integration. Substituting Eqs. (15)–(17) into Eq. (14) gives

$$\int_0^l \Phi(s_\theta)[K_1(r_{p_\theta}) + K_2(r_{p_\theta})]\hat{f}\,ds_\theta - \Phi(s_p)\int_0^l [F_1(r_{p_\theta}) + F_2(r_{p_\theta})]\hat{f}\,ds_\theta$$
$$- \int_0^l v(s_\theta)[I_1(r_{p_\theta}) + I_2(r_{p_\theta})]\hat{f}\,ds_\theta = 2\pi[\Phi(s_p) + \alpha v(s_p)] \ , \tag{18}$$

where l is the length of the generating line of the surface of revolution. The s-θ coordinate directions have now been essentially uncoupled so that the problem has been reduced to the evaluation of the line integrals in the coordinate directions on the surface of the body. This formulation does not restrict the form or type of boundary conditions on the body; it merely assumes that the boundary conditions can be represented by a sum (expanded in a set) of tangential modes.

II. RESULTS

The acoustic fields for a sphere, cylinder, and inlet configuration have been computed by numerical solution of Eq. (18) using the techniques described in Ref. 11. Basically, this method consists of first specifying the $\rho - z$ coordinates and the normal vector at each point on the surface. From these quantities the distances and the normal derivatives can be obtained. The integral in Eq. (18) is then separated into n integrals taken over subintervals of length l/n. The acoustic potential is assumed constant over each subinterval and the integrations are performed numerically using Gauss-Legendre quadrature in the $\rho - z$ plane. Over the subinterval containing the point P, the integrand in Eq. (18) becomes infinite since r_{p_θ} approaches zero. Thus, only an even number of points is used in the quadrature algorithim,

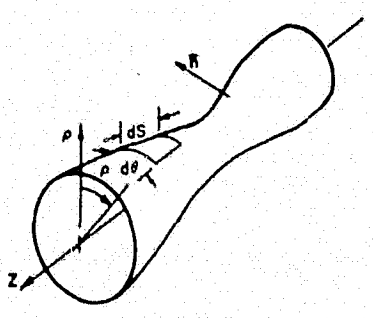

FIG. 2. Cylindrical surface geometry.

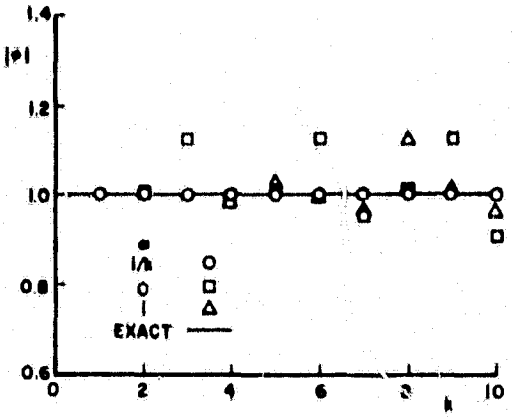

FIG. 3. Effect of the coupling constant on the computed surface potential for a sphere of unit radius with 20 subintervals.

since an odd number would necessitate inclusion of the point where $r_{p_\theta} = 0$. A Gauss–Legendre quadrature formula is used in the circumferential direction to evaluate Eqs. (15)–(17). All calculations were performed on the Georgia Tech CDC Cyber 70/74 with 16 significant figures.

In all geometries investigated, exact solutions were obtained for $m = 0$ by assuming a monopole source located at point $(\rho, z) = (0, 0)$ inside the surface. The normal velocities and/or admittance values are then computed at each point on the surface using Eq. (6) and taken as the boundary conditions in Eq. (18). The surface potential $\Phi(s_p)$ is then computed from Eq. (18) and the farfield potential is obtained by numerically solving Eq. (2) with Eq. (6). The computed surface and farfield potentials are then compared with the known potential distribution of the monopole source

$$\varphi(P) = -e^{ika}/a \ , \tag{19}$$

where a is the distance from the source to the observation point. For $m = 1$ a dipole source was used to generate exact solutions, and for $m = 2$ a quadrapole source was used.

To investigate the effect of the coupling constant α in Eqs. (15)–(17), the surface potential distributions for a sphere of unit radius with a uniformly vibrating surface (i.e., $m = 0$) were computed for $\alpha = 0$, i, and i/k. Twenty subintervals were taken in the $\rho - z$ plane, a four-point Gauss–Legendre quadrature formula was used over each subinterval and a 20-point Gauss–Legendre formula was used in the θ direction. The magnitude of the potential should be unity at all points on the surface. The results presented in Fig. 3 show the computed magnitudes of the surface acoustic potential to be in error by 12% for $\alpha = 0$ at nondimensional wavenumbers ka close to π, 2π, and 3π. These results are those that would be obtained from Eq. (7). The relatively large errors are expected from the analysis of Burton and Miller[4] and from previous investigations using Eq. (7).[2,5] Burton proves that setting the imaginary part of α nonzero guarantees unique solutions to Eq. (18), For $\alpha = i$ the maximum error is reduced to less than 4% except when k is close to 8.0. However, when $\alpha = i$, and for sufficiently high values of ka, Eq. (9) is dominated by terms arising from

TABLE I. Effect of the coupling parameter α on the computed values of the surface potential for a sphere. On the surface $A(Q)=(1-ik)e^{ik}$, $Y(Q)=0$, $\varphi_{exact}^{(Q)}=-e^{ik}=$constant, $m=0$. All values of ka correspond to internal eigenfrequencies. Twenty subintervals were taken in the p-z plane.

ka \ α		0	i/k	i	Exact
π	φ_r	2.0	1.000	0.998	1
	φ_i	−0.3	0.001	−0.012	0
4.493409	φ_r	0.190	0.217	0.308	0.217
	φ_i	0.979	0.976	0.955	0.976
2π	φ_r	−2.0	−1.000	−0.996	−1
	φ_i	12.6	0.000	0.031	0
7.725252	φ_r	−0.081	−0.128	−0.400	−0.128
	φ_i	−0.994	−0.992	−0.872	−0.992
3π	φ_r	2.0	1.000	0.995	1
	φ_i	−19.0	0.000	−0.050	0

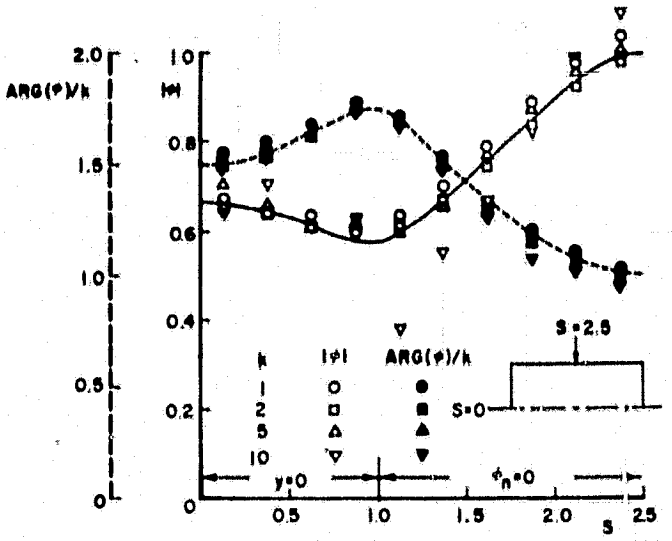

FIG. 5. Effect of discontinuous boundary conditions on the accuracy of the computed surface potential for a cylinder.

Eq. (8). As a result, the solution equations become ill-conditioned when ka is sufficiently high and close to one of the eigenfrequencies associated with the integral equation based on Eq. (8). In Table I computed values close to these eigenfrequencies and the eigenfrequencies of Eq. (7) are compared with exact results for $\alpha=0$, i, and i/k. In all case, the value of i/k gives the most accurate results. In Table II, the effect of introducing an admittance condition is presented for $\alpha=i/k$. The admittance $Y(Q)$ and forcing function $A(Q)$ in Eq. (6) are chosen so that the relations

$$\frac{\partial\varphi}{\partial n_q}-Y(Q)\varphi=A(Q)\ ;\quad \varphi=\frac{-e^{ikr}}{r}\ , \tag{20}$$

are satisfied on the surface and the exact solutions can be readily computed. The loss in accuracy when an admittance condition is used is minimal and restricted to the third significant figure. However, for discontinuous boundary conditions, where the forcing function is specified over one part of the surface (i.e., the admittance is zero there) and the admittance is specified over the remaining surface, errors of over ten percent in the real and imaginary parts of the computed surface potential result. For comparison, the case of a constant forcing function and admittance over the sphere for $\alpha=0$ is also presented and in all cases yields results of less accuracy than those obtained with $\alpha=i/k$.

In this study consistently good results were obtained with $\alpha=i/k$. In Fig. 3 the computed and exact values for $\alpha=i/k$ agree to three significant figures over the range of nondimensional wavenumbers from one to ten. In fact, for this value of α, the accuracy is significantly better at all wavenumbers investigated. While Burton and Miller[4] provide no recommendations for choosing one value of α over any other value with an imaginary component, the choice $\alpha=i/k$ used in the present study can be explained as follows. The terms in Eqs. (15)–

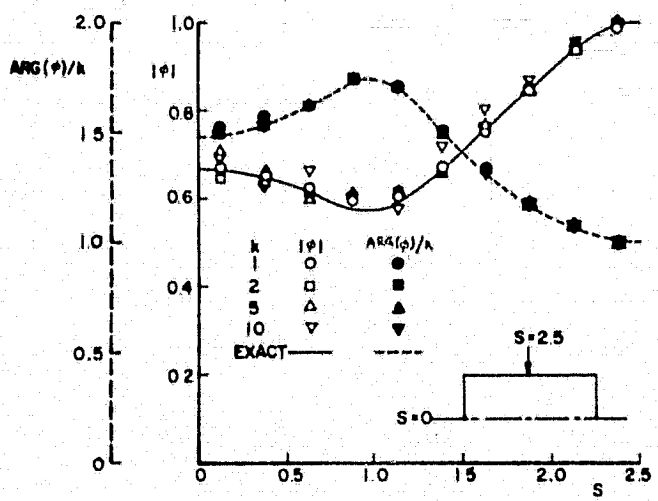

FIG. 4. Dependence of the computed surface potential for a finite cylinder with a zero admittance and nonzero normal velocity everywhere on the surface for 20 subintervals.

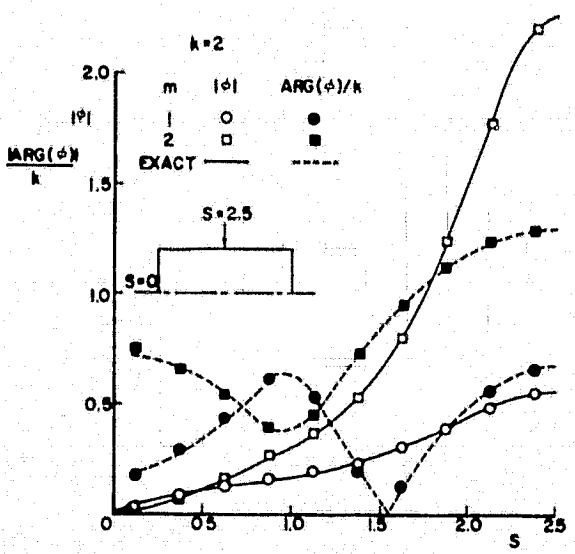

FIG. 6. Computed surface potential for a cylinder at the first and second tangential modes for $ka=2$.

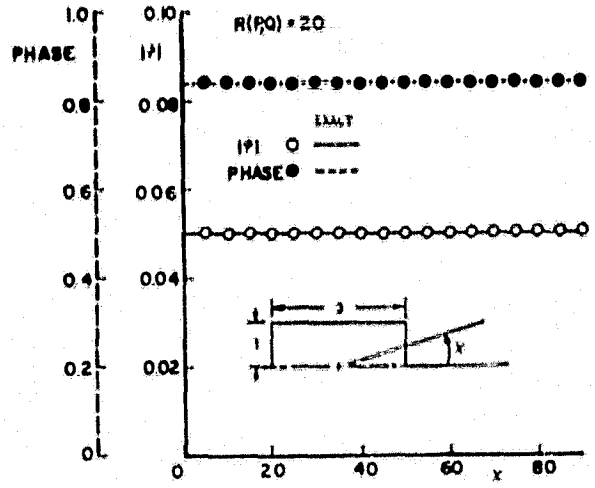

FIG. 7. Computed farfield potential distribution for a cylinder at $k=2$, $m=0$, and 20 radii from the center.

(17) which involve α are of order k^2, whereas the remaining terms are of order k. Therefore, at higher wavenumbers the terms of order k^2 dominate. By choosing α to vary inversely with the wavenumber, all terms in Eqs. (15)–(17) remain of the same order with respect to wavenumber.[12]

A problem of more practical importance is the finite axisymmetric duct since this surface approximates an engine configuration. The surface potential distributions are presented in Fig. 4 at different nondimensional wavenumbers for $m=0$. The normal acoustic velocity distribution $A(Q)$ is chosen so that the solution for the acoustic potential satisfies Eq. (19). The parameter α is taken to be i/k. Twenty subintervals are taken in the $\rho-z$ plane and a 20-point Gauss–Legendre quadrature is used in the θ direction. In Fig. 4 the variations of the magnitude and phase with distance along the perimeter s are presented. The largest errors in the computed magnitude of the potential of about 10% occur on the ends of the cylinder and at the corners. The results at the ends can be improved without increasing the number of points by area weighting rather than taking equidistant points along the perimeter. The errors in the phase are less than 4% in all cases. The errors in the magnitude of the computed surface potential increase with increasing nondimensional wavenumber, but, even when $ka=10$, the numerical results are within 10% of the exact solutions. For $\alpha=0$ or i the errors are significantly larger above $ka=2$.

In most inlet problems the boundary conditions are discontinuous with the acoustic velocity or potential (which is directly proportional to the acoustic pressure) specified over part of the surface and the admittance (representing liners) over the rest. To determine the effect of the discontinuities and the use of an admittance function on the numerical results for $m=0$, a cylinder was investigated. The velocity was specified on the ends and the admittance was specified in the center so that the solution for Φ was given by Eq. (19) and Eq. (6) is satisfied. Again, 20 points are used in the $\rho-z$ and θ directions. The results are shown in Fig. 5. Although the errors in the numerical results for this case are higher than those observed in Fig. 4, the errors still remain within 10% for values of ka less than 5. However, when $ka=10$ errors of up to 40% in the magnitude of the potential are encountered close to the discontinuity in the boundary condition. This error can be reduced by increasing the number of subintervals in the $\rho-z$ plane. Doubling the number of subintervals halves the error. When both the normal acoustic velocity and the admittance are continuous on the surface, the errors are of the same order of magnitude as those of Fig. 4. For tangential modes, the variation in the circumferential direction behaves as $\cos m\theta$ where $m=1,2,\ldots$. To check the numerical integration scheme in the circumferential direction, the surface acoustic potential was

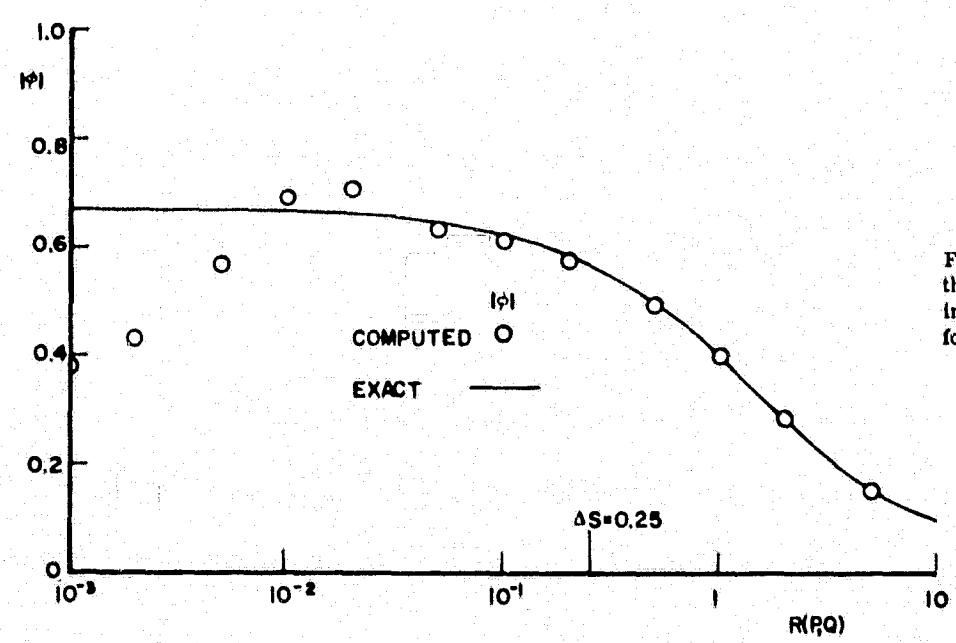

FIG. 8. Dependence of the accuracy of the computed farfield solution of a cylinder upon the distance from the surface for $k=2$ and $m=0$.

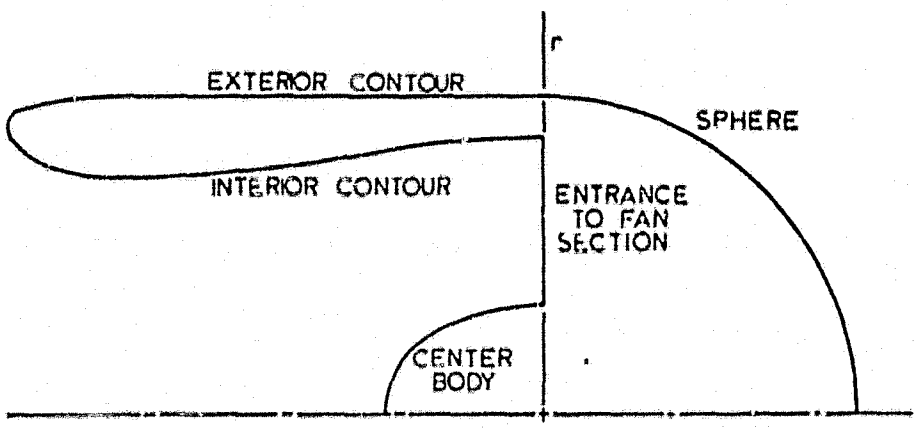

FIG. 9. Inlet geometry.

computed for $m=1$ and $m=2$ for the cylinder shown in Fig. 4. The results are presented in Fig. 6 for $ka=2$ with the normal acoustic velocity specified everywhere on the surface. The computed and exact results (i.e., from a dipole and quadrapole) are in agreement to within 2% for both $m=1$ and $m=2$.

It has been shown[5] that once the surface potential has been accurately computed, the farfield can be determined to at least the same accuracy as the surface potential. This result is confirmed by the data presented in Fig. 7 for the cylinder of Fig. 4 with the velocity specified everywhere on the surface with $ka=2$ and $m=0$. The results at 20 radii from the surface are in agreement with exact results obtained from Eq. (19) to within 1% even though the surface errors at some points are above 2%. Data in Fig. 8 show that accurate results are obtained at distances greater than one integration stepsize from the surface. At closer distances errors from the numerical evaluation of the singularity in the Green's function defined by Eq. (4) leads to large errors.

The studies of the acoustic fields of the sphere and cylinder served to check out and refine the numerical procedures and programming techniques. The next configuration investigated was an inlet used in a study by NASA.[13] This inlet is shown in Fig. 9 and was chosen because:

(1) unlike most inlets used in research studies, it does not have a bell-mouth shape but is shaped like a typical inlet used in existing aircraft, and

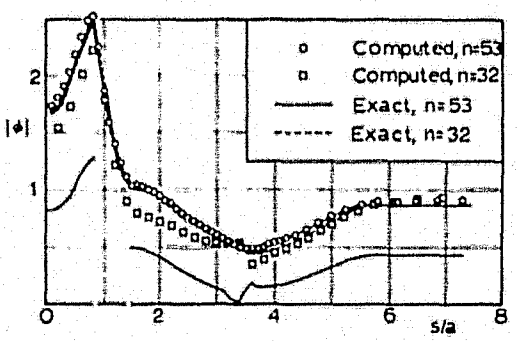

FIG. 10. Effect of increasing the number of subintervals in computing the surface potential for the inlet configuration at $ka=1$, $m=0$.

(2) complete details on generating the inlet boundary are given in Ref. 13. For this inlet, all cases were investigated with $\alpha=i/k$.

As seen in Fig. 10, the normal velocity distribution, which represents a forcing function, is highly discontinuous and provides a severe test of the numerical techniques employed. The numerical and exact solutions for the surface acoustic potential are compared in Fig. 10 for 32 and 54 subintervals taken along the perimeter of the inlet in the $\rho-z$ plane. Because of the errors in approximating the lengths of each subinterval, the exact solutions differ slightly as the distance along the perimeter s increases. The centerbody in Fig. 9 extends from $0\leq s\leq 0.8$, the fan inlet covers $0.8\leq s\leq 1.4$, the interior contour extends from $1.4\leq s\leq 3.5$, the exterior from $3.5\leq s\leq 5.5$, and the circular arc lies within the interval $5.5\leq s\leq 7.45$. Increasing the number of points decreases the error proportionately as indicated by the data in Fig. 10 at a nondimensional wavenumber ka of unity, where a is the radius of the inlet at the fan entrance section. The absolute average error in the results decreases from 10.2% for 32 subintervals to 4.16% for 53 subintervals. The computation time increased from 53 to 143 s, respectively.

TABLE II. Effect of specifying an admittance on the computed surface potential for a sphere. In all cases $m=0$, twenty subintervals are taken in the $\rho-z$ plane, and $\varphi_{\text{exact}}=-e^{ik}$ everywhere on the surface. For Case I, $A(Q)=e^{ik}$ and $Y(Q)=0$ everywhere on the surface. For case III, $A(Q)=e^{ik}(1-ik)$ and $Y(Q)=0$ over 1/5 of the surface and $A(Q)=0$, $Y=(1-ik)$ over the remainder. Case II is considered in Table I.

ka		Case I $\alpha=i/k$	Case I $\alpha=0$	Case II $\alpha=i/k$	Case III $\alpha=i/k$	Exact values
1	φ_r	−0.539	−0.537	−0.538	−0.52	−0.540
	φ_i	−0.845	−0.849	−0.843	−0.87	−0.842
2	φ_r	0.418	0.422	0.417	0.43	0.416
	φ_i	−0.911	−0.937	−0.909	−0.92	−0.909
3	φ_r	0.993	0.916	0.990	1.00	0.990
	φ_i	−0.142	−0.496	−0.140	−0.16	−0.141
5	φ_r	−0.285	−0.288	−0.284	−0.25	−0.284
	φ_i	0.961	1.145	0.959	1.00	0.959
10	φ_r	0.841	−0.3	0.839	0.90	0.839
	φ_i	0.546	0.9	0.544	0.49	0.544

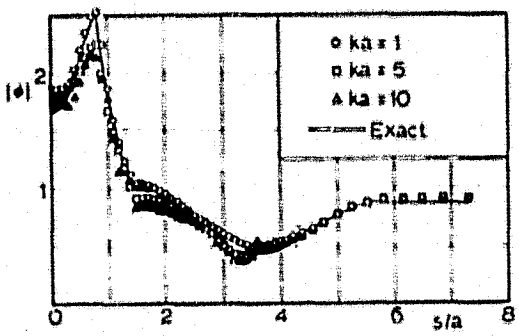

FIG. 11. Effect of increasing frequency for the inlet configuration at $m=0$, $n=53$ on the computed surface potential.

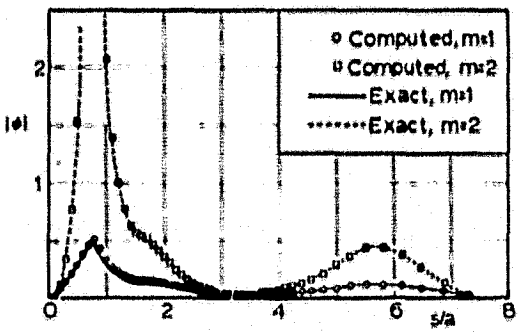

FIG. 12. Effect of mode number m on the computed surface potential of the inlet configuration for $ka=2$ and $n=53$.

As shown in Fig. 11, the errors increase with increasing frequency. Like the cylinder, the maximum error in the acoustic potential for the inlet configuration occurs at the points of discontinuity. The average error increases from 4.16% at $ka=1$ to 15% at $ka=10$.

For the data in Figs. 10 and 11, the acoustic potential is assumed constant in the tangential plane. The results for a $\cos(m\theta)$ distribution are presented in Fig. 12 at $ka=2$. These results show the insensitivity of the accuracy of the computed results to the tangential distribution for $m=1,2$. The exact solutions were again generated by assuming dipole and quadrapole sources located at $(\rho,z)=(0,0)$.

Based on the above results our numerical and programming techniques are capable of yielding reliable results for arbitrary geometries and boundary conditions. At higher frequencies, ($ka>5$) it appears that more points must be taken to increase the accuracy of the computed results.

III. SUMMARY AND CONCLUSIONS

An integral solution of the Helmholtz equation is developed for use in acoustic radiation problems. Unlike the classical formulation which can lead to integral equations that do not have unique solutions at frequencies corresponding to certain internal eigenfrequencies of the region enclosed by the surface under consideration, the formulation used in this study is valid at all frequencies. Also, unlike most current methods and formulations it is straightforward to implement regardless of how complicated the surface or the boundary conditions may be. The surface potentials computed numerically for a sphere and cylinder using 20 subintervals along the perimeter and for an inlet configuration with 53 subintervals are accurate to within 10% for nondimensional wavenumbers ka of from one to ten, where k is the wavenumber and a is the characteristic length. For discontinuous boundary conditions, the numerical and exact values are in agreement to within 10% for $ka<5$. At higher frequencies the results are as much as 40% in error at points of discontinuity, which suggests taking more points in evaluating the integral equation to increase the accuracy when discontinuous boundary conditions are specified. Increasing the number of subintervals decreases the error proportionately. At distances greater than the numerical integration stepsize, the farfield results are at least as accurate as the corresponding surface potential solutions.

Note added in proof: We wish to thank Dr. P. J. T. Filippi for drawing our attention to the following paper: P. J. T. Filippi, "Layer Potentials and Acoustic Diffraction," J. Sound Vib. **54**, 473–500 (1977).

ACKNOWLEDGMENT

This work was supported by the AFOSR under Contract Number F49620-77-C-0066, Lt. Col. Lowell Ormand project monitor.

[1]A. J. Burton, "The Solution of Helmholtz' Equation in Exterior Domains using Integral Equations," NPL Report NAC 30, National Physical Laboratory, Teddington, Middlesex, Jan. 1973.
[2]H. A. Schenck, "Improved Integral Formulation for Radiation Problems," J. Acoust. Soc. Am. **44**, 41–58 (1968).
[3]F. Ursell, "On the Exterior Problems of Acoustics," Proc. Cambridge Philos. Soc. **74**, 117–125 (1973).
[4]A. J. Burton and G. F. Miller, "The Application of Integral Equation Methods to the Numerical Solutions of Some Exterior Boundary Value Problems," Proc. R. Soc. London A **323**, 201–210 (1971).
[5]W. L. Meyer, W. A. Bell, M. P. Stallybrass, and B. T. Zinn, "Boundary Integral Solutions of Three Dimensional Acoustic Radiation Problems," J. Sound Vib. **59**, 245–262 (1978).
[6]P. M. Morse and K. U. Ingard, *Theoretical Acoustics* (McGraw-Hill, New York, 1969), Chap. 7.
[7]It has been pointed out to us by a reviewer that an equation of the same general form as Eq. (9) has been given by Chertock.[8] However, for an arbitrary, smooth surface, Chertock did not interpret this integral equation correctly. Specifically, the limit indicated in the final term of (A17), Ref. (8) does not exist, as may be verified for the simple case of a sphere.
[8]Chertock, "Integral Equation Methods in Sound Radiation and Scattering from Arbitrary Surfaces," David W. Taylor, Naval Ship Research and Development Center Report 3538, June, 1971
[9]M. P. Stallybrass, "On a Pointwise Variational Principle for the Approximate Solution of Linear Boundary Value Problems," J. Math. Mech. **16**, 1247–1286 (1967).
[10]G. Chertock, "Sound Radiation from Vibrating Surfaces," J. Acoust. Soc. Am. **36**, 1305–1313 (1964).
[11]W. A. Bell, W. L. Meyer, and B. T. Zinn, "Predicting the Acoustics of Arbitrarily Shaped Bodies Using an Integral Approach," AIAA J. **15**, 813–820 (1977).
[12]It is interesting to note that in his report Chertock[8] suggests the use of $1/k$ on the grounds that it has the correct physical dimensions (i.e., length) that will maintain the dimensional homogeneity of Eq. (18).
[13]B. A. Miller, B. J. Dastoli, and H. L. Wo~~r~~esky, "Effect of Entry-Lip Design on Aerodynamics and Acoustics of High-Throat-Mach-Number Inlets for the Quiet, Clean, Short-Haul Experimental Engine," NASA TM X-3222, 1975.

References

1) "Predicting the Acoustics of Arbitrarily Shaped Bodies Using an Integral Approach." W. A. Bell, W. L. Meyer and B. T. Zinn, AIAA Journal, Vol. 15, No. 6, pp. 813-820, June 1977.

2) "Boundary Integral Solutions of Three Dimensional Acoustic Radiation Problems," W. L. Meyer, W. A. Bell, M. P. Stallybrass and B. T. Zinn, Journal of Sound and Vibration, Vol. 59, No. 2, pp. 245-262, July 1978.

3) "Prediction of the Sound Field Radiated from Axisymmetric Surfaces," W. L. Meyer, W. A. Bell, M. P. Stallybrass and B. T. Zinn, Journal of the Acoustical Society of America, Vol. 63, No. 2, pp. 631-638, March 1979.

4) "Effect of Entry-Lip Design on Aerodynamics and Acoustics of High-Throat-Mach-Number Inlets for the Quiet, Clean, Short-Haul Experimental Engine," B. A. Miller, B. J. Dastoli and H. L. Wesoky, NASA TM X-3222, Lewis Research Center, Cleveland, Ohio, May 1975.

5) "Noise Suppression in Jet Inlets," B. T. Zinn, W. L. Meyer and W. A. Bell, AFOSR Annual Technical Report, AFOSR-TR-79-0614, Contract No. F49620-77-C-0066, February, 1979.

6) "Noise Suppression in Jet Inlets," B. T.Zinn, W. L. Meyer and B. R. Daniel, AFOSR Final Technical Report, AFOSR- 80-0452 , Contract No. F49620-77-C-0066, February, 1980.

7) Handbook of Mathematical Functions with Formulas, Graphs, and Mathematical Tables, edited by M. Abramowitz and I. A. Stegun, Dover Publacations, Inc., N. Y., Fifth Edition, 1968, (Chapter 25).